

**Synthesis and Characterization of Nanostructured  
Nickel Cobalt Sulfide/MWCNTs Composite  
Grown on Nickel Foam as Direct Electrode  
Material for Supercapacitor**



**By**

**Muhammad Saleem Akhter**

**School of Chemical and Materials Engineering (SCME)  
National University of Sciences and Technology (NUST)**

**2019**

# **Synthesis and Characterization of Nanostructured Nickel Cobalt Sulfide/MWCNTs Composite Grown on Nickel Foam as Direct Electrode Material for Supercapacitor**



Name: Muhammad Saleem Akhter  
Reg. No: 00000172297

**This thesis is submitted as a partial fulfillment of the requirements for the degree of  
MS in Nanoscience and Engineering**

**Supervisor Name: Dr. Iftikhar Hussain Gul**

**School of Chemical and Materials Engineering (SCME)  
National University of Sciences and Technology (NUST)**

**H-12 Islamabad, Pakistan**

**May, 2019**

## **Dedication**

My humble efforts for this dissertation and all of my academic achievements are dedicated to my father, Mr. Zulfiqar Khan, whose example evolved me to think about character, values, resilience, grit, patience and determination. Which were the skills that actually helped me to navigate my life and develop myself intellectually and personally.

My mother, who's continuous support, encouragement, love, and prayers of days & nights made me able to get success and honor. Most importantly my brother Muhammad Akbar for educating me with affection & adoration and their dedicated partnership for my success. Few of my close friends, who taught me to concentrate on the positive in life and use the talents God gave me.

Along with all hard working and respected teachers, especially my research instructor Dr. Iftikhar Hussain Gul who has been a constant source of knowledge and motivation.

## Acknowledgements

Above all, I am gratifying to Allah for benevolent me patience, strength, enlightenment and fortuity to endeavor this research and accomplish it competently.

Supremely, I would like to thanks my research instructor **Dr. Iftikhar Hussain Gul** for providing valuable guidance, supervision, mentoring and encouragement.

I also thanks **Dr. Taqi Mehran** for providing valuable comments, support and guidance through the research. Candid thanks to the staff and management of **SCME (NUST)** for providing me liberty to enhance my career and establishing this research.

I also like to direct my deepest gratefulness to **Dr. Aftab Akram** and **Dr. Zakir Hussain** for being on my thesis guidance. I am extremely thankful to my research fellow **Mr. Ahmad Ali, Mr. Arman Liaqat and Mr. Mutawara Baig** for providing me necessary technical suggestions during my research pursuit.

The involvement of all above have been very important in carrying out this research.

## Abstract

The synthesis of NiCo<sub>2</sub>S<sub>4</sub>/MWCNTs composite on Ni foam and its applications were investigated. A hydrothermal method involving two steps is used in this work for the insitu decoration of NiCo<sub>2</sub>S<sub>4</sub>/MWCNTs composite on bare nickel foam. Nanostructures of NiCo<sub>2</sub>S<sub>4</sub> are also synthesized via same route. The synthesized samples were characterized through versatile techniques such as XRD for structural and SEM for morphological studies. The electrochemical analysis of the materials is performed using CV and GVD tests. A typical three electrode method is used for the electrochemical measurement in a 2 M KOH electrolyte. The calculated areal capacitance at the current density of 3 mA cm<sup>-2</sup> was 5.38 F cm<sup>-2</sup> and mass specific capacitance was 2210 F g<sup>-1</sup>. As the current density is increased, the areal capacitance was decreased. The mixture of high electrical conductivity, open structure of MWCNTs and the nickel, cobalt played a noteworthy parts to get supercapacitor electrodes with exceptional performance. Cyclic stability test conducted revealed that new composite material has good electrochemical performance.

# Table of Contents

<b>Chapter No.1</b> .....	1
<b>Introduction</b> .....	1
1.1 Energy storage devices.....	2
1.1.1 Capacitors.....	2
1.1.2 Batteries.....	4
1.1.3 Fuel Cells .....	5
1.3. Supercapacitors .....	7
1.4. Comparison of state of the art energy storage devices.....	8
1.5. Super capacitor applications .....	9
1.7. Research objectives.....	10
1.8. Dissertation organization .....	10
<b>Chapter N0.2</b> .....	12
<b>Literature Review</b> .....	12
2.1 Emergence of Super capacitor.....	12
2.2 Supercapacitors principle .....	13
2.3 An Electrochemical double layer .....	14
2.4 Pseudocapacitance.....	15
2.5 Types of supercapacitors .....	16
2.6 ECPs based ultracapacitors .....	16
2.6.1 Polyaniline .....	17
2.6.2 Polypyrrole based ultracapacitors .....	18
2.6.3 Polythiophene based ultracapacitors .....	19
2.7 Carbon based composite electrode materials .....	20
2.7.1 Carbon nanotubes as an electrode materials .....	20
2.7.2 Graphene based electrode materials.....	21

2.7.3 Activated carbon .....	21
2.8 Metal oxide based ultracapacitors .....	23
2.8.1 Binary MO <sub>x</sub> based electrode materials .....	24
2.9 Metal sulfides based ultracapacitors .....	25
2.9 Challenges .....	26
2.10 Current efforts and future advancement.....	27
<b>Chapter No.3</b> .....	329
3.1 Methods and materials .....	29
3.1.1 Synthesis of NiCo <sub>2</sub> S <sub>4</sub> nanostructures .....	30
3.1.1a Synthesis of metal hydroxide precursor .....	30
3.1.1b Synthesis of sulfides.....	31
3.1.2. Insitu decoration of MWCNTs and NiCo <sub>2</sub> S <sub>4</sub> nanostructures on Ni foam	32
3.2 Characterizations.....	35
3.2.1 Investigation of Morphology.....	35
3.2.2 Microstructure Characterization.....	37
3.3 Electrochemical Properties .....	40
3.3.1 Cyclic Voltammetry .....	40
3.3.1.1 Definition of important electrochemical terms. ....	41
3.3.1.2. Schematic illustration of CV system and principle of operation .....	42
3.3.2. Galvanostatic charge-discharge (GCD) .....	44
<b>CHAPTER No.4</b> .....	47
4 Results and Discussion.....	47
4.1 Electrochemical performance of supercapacitors, its challenges and possible potential remedies. ....	47
4.2 Morphological analysis of nanostructures.....	47
4.2.1 Morphological analysis of NiCo <sub>2</sub> S <sub>4</sub> .....	47
4.2.2 Morphological studies of NiCo <sub>2</sub> S <sub>4</sub> /MWCNTs composite.....	48

4.3 Phase and structural analysis .....	49
4.4 Electrochemical studies of NiCo <sub>2</sub> S <sub>4</sub> and NiCo <sub>2</sub> S <sub>4</sub> /MWCNTs composite .....	51
4.4.1 Cyclic voltammetry of NiCo <sub>2</sub> S <sub>4</sub> and its nanocomposite .....	51
4.4.2 GCD test .....	56
<b>5 Conclusions.....</b>	<b>63</b>



## List of Figures

Figure 1.1 Up-to date energy storage devices .....	2
Figure 1.2 Illustration of supercapacitor [12] .....	4
Figure 1.3 Schematic of Li-ion battery [14].....	5
Figure 1.4 Schematic of fuel cell [15].....	6
Figure 1.5 Energy flow diagram .....	6
Figure 1.6 Electrochemical performance of different storage devices [12].....	8
Figure 1.7 Schematic showing applications of supercapacitor [13] .....	9
Figure 2.1 Schematic of supercapacitors function [19] .....	14
Figure 3.1 Flow chart of the synthesis process & characterizations .....	29
Figure 3.2 Schematic diagram of different synthesis steps of metalhydroxide nanostructures on Ni foam .....	30
Figure 3.3. Metal hydroxide nanostructures deposited on the nickel foam .....	31
Figure 3.4 Schematic diagram of different synthesis steps of NiCo <sub>2</sub> S <sub>4</sub> .....	31
Figure 3.5 Optical view of NiCo <sub>2</sub> S <sub>4</sub> /MWCNTs on Ni foam.....	32
Figure 3.6 Teflon-lined stainless-steel autoclave.....	33
Figure 3.7 Muffle Furnace .....	34
Figure 3.8 Schematic working of SEM [113] .....	36
Figure 3.9 Scanning Electron Microscopy (SEM) (Model: JEOL JSM-6490A).....	37
Figure 3.10 Schematic diagram of an XRD unit [115] .....	38
Figure 3.11 Bragg's Law, working Principle of XRD [116] .....	39
Figure 3.12 XRD Spectrometer (model D8-ADVANCE).....	40
Figure 3.13 Representation of three electrode system employed in CV [118] .....	42
Figure 3.14 Cyclic voltammetry curve generation [118].....	43
Figure 3.15 Current as a function of time [118].....	43
Figure 3.16 Typical cyclic voltamogram [118].....	44
Figure 3.17 Schematic of Bio Logic VSP instrument used for electrochemical measurements. ....	45
Figure 4.1 (a) SEM image of bare nickel foam (b) loaded with nanostructures (c), (d) shows NiCo <sub>2</sub> S <sub>4</sub> nanostructures. ....	48
Figure 4.2 SEM images of nickel foam loaded with NiCo <sub>2</sub> S <sub>4</sub> /MWCNTs.....	49
Figure 4.3 XRD patterns of NiCo <sub>2</sub> S <sub>4</sub> , NiCo <sub>2</sub> S <sub>4</sub> /MWCNTs and bare Ni foam.....	50
Figure 4.4 Cyclic voltamogram curve of bare nickel foam. ....	52

Figure 4.5 CV curves of NiCo <sub>2</sub> S <sub>4</sub> at different scan rates .....	52
Figure 4.6 CV curves of the NiCo <sub>2</sub> S <sub>4</sub> /MWCNTs nanocomposite .....	53
Figure 4.7 Cyclic voltamogram of NiCo <sub>2</sub> S <sub>4</sub> and NiCo <sub>2</sub> S <sub>4</sub> /MWCNTs. ....	54
Figure 4.8 Max current vs potential scan rate for NiCo <sub>2</sub> S <sub>4</sub> and NiCo <sub>2</sub> S <sub>4</sub> /MWCNTs	55
Figure 4.9 GCD curves for NiCo <sub>2</sub> S <sub>4</sub> /Ni foam.....	56
Figure 4.10 GCD curves for NiCo <sub>2</sub> S <sub>4</sub> /MWCNTs/Ni foam.....	57
Figure 4.11 GCD comparison curves for NiCo <sub>2</sub> S <sub>4</sub> and NiCo <sub>2</sub> S <sub>4</sub> /MWCNTs .....	57
Figure 4.12 Galvanostatic discharge curves for NiCo <sub>2</sub> S <sub>4</sub> at different densities.....	58
Figure 4.13 Galvanostatic discharge curves of NiCo <sub>2</sub> S <sub>4</sub> at different current rates ....	59
Figure 4.14 Galvanostatic discharge curves of NiCo <sub>2</sub> S <sub>4</sub> and NiCo <sub>2</sub> S <sub>4</sub> /MWCNTs ....	59
Figure 4.15 showing the mass specific capacitance at different current densities.....	60
Figure 4.16 Areal capacitance vs current density .....	61
Figure 4.17 the cycling performance of NiCo <sub>2</sub> S <sub>4</sub> /MWCNTs/Ni and NiCo <sub>2</sub> S <sub>4</sub> /Ni electrodes at the current density of 20 mA cm <sup>-2</sup> . ....	62

## List of Abbreviations

<b>NiCo<sub>2</sub>S<sub>4</sub> NSs</b>	Nickel cobalt Sulfide Nanostructures
<b>PEG</b>	Polyethylene glycol
<b>DMF</b>	Dimethyl form amide
<b>ECPs</b>	Electrically conductive polymers
<b>CC</b>	Carbon Cloth
<b>NC</b>	Nano composite
<b>MO<sub>x</sub></b>	Metal oxide
<b>PPy</b>	Polypyrrole
<b>PANI</b>	Polyaniline
<b>PTh</b>	Polythiophene
<b>NSs</b>	Nano structures
<b>GCE</b>	Glassy carbon electrode
<b>GCD</b>	Galvanostatic charge-discharge
<b>CV</b>	Cyclic Voltammetry
<b>XRD</b>	X-Ray Diffraction
<b>SEM</b>	Scanning Electron Microscopy

# Chapter No. 1

## Introduction

The enormous increase in world residents and running down of fossil fuels, there is an exigent need to improve hygienic and efficient renewable energy sources, as well as the new approaches to convert and store energy. Many renewable energy sources, like wind energy and solar, have growing energy creation in recent years, but sun does not shine at nights and all days, and storm does not tide on our demands. Electrochemical energy storage has fascinated more and more consideration [1, 2]. In the recent years considerable effort were made to the enlargement of fuel cells and Li-ion batteries however their lesser life cyclability and high production cost has mired their deployment in practical applications [3-5]. Supercapacitors, also known as ultra-capacitors having fast charging and discharging potential and life cyclability have become favorable applicants for energy storage applications [6]. The very first approach about supercapacitors was based on carbonaceous material having extremely high surface area and the first patent awarded in the field of supercapacitors was in 1957. Using tetra-alkyl ammonium salt as electrolytic medium in 1969, SOHIO marketed the first carbon based energy storing device and one year later in 1970 he went for patent a plate like capacitor using carbon paste saturated in electrolyte [6]. Supercapacitors also called ELDC enable us to merge the benefits of high energy density of battery and high power density of capacitors [7, 8]. EDLC are crucial components of advance hybrid automobiles, electronic gadgets, portable electronics, memory storage systems, industrial power management, electrical telecommunication systems there by providing high power output [9, 10]. Energy storage in supercapacitors is based on formation of double layer (EDL). Capacitance is due to adsorbed ions and pseudocapacitance results from redox reactions. Pseudocapacitors developed with metal oxides or conducting polymers as active electrode material, although delivered a high capacitance, but could not maintain this capacitive performance for a long period of cycling. Contrarily, EDL capacitors can undergo a million of charge-discharge cycles but have lower capacitance compared to Pseudocapacitors [11].

At present, three important energy storage devices batteries, capacitors and fuel cell are being commercialized.

## 1.1 Energy storage devices

A schematic representation of the energy storage devices is given in figure 1.1.

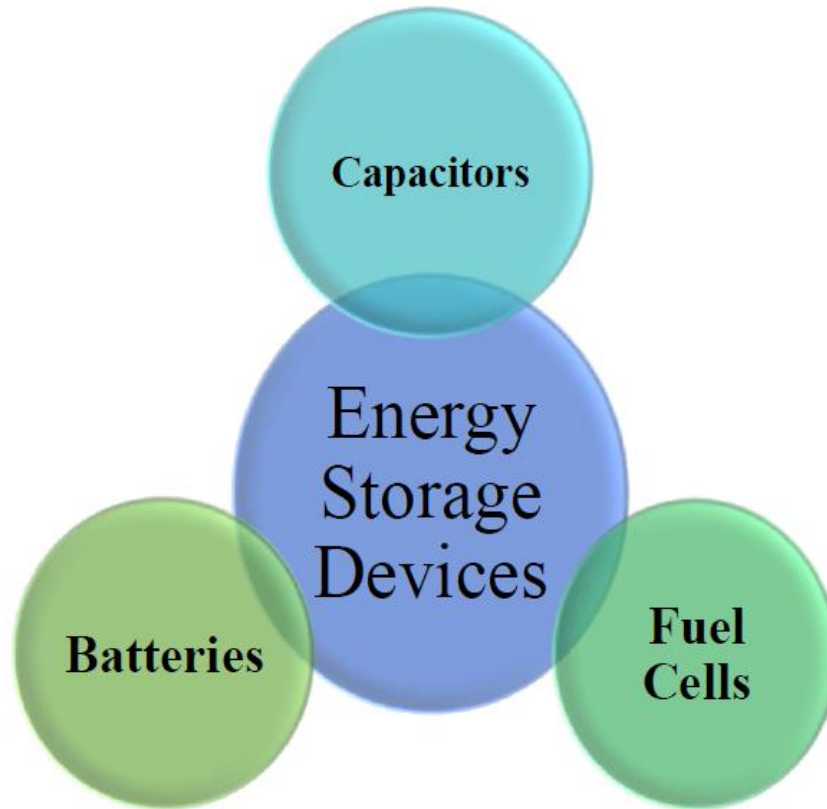


Figure 1.1 Up-to date energy storage devices

### 1.1.1 Capacitors

Capacitor, a passive electrical device that can store electrical energy as a result of charges in an electric field among two conducting plates referred as electrodes. Capacitors are capable of releasing the stored energy reasonably fast resulting in a high output, but its performance is limited by the energy density as it cannot store greater amount of energy to account for a high energy density in comparison with electro chemical batteries. Traditional capacitors, also called electrostatic capacitors, generally comprise of two electrodes, parted by an inner insulating layer called a dielectric, as shown in figure 1.2[12]. When a power source is applied to a capacitor, charges gather on the surfaces of the conducting electrodes, divided by insulator resulting in an electric field between the electrodes. This electric field generated across the electrodes enables the device to store electrical energy.

An important parameter used to characterize capacitors is its capacitance  $C$ , which can be simply defined as the total amount of charge  $Q$  stored divided by applied potential  $V$ .

$$C = \frac{Q}{V} \quad (1.1)$$

Here  $C$  denotes the capacitance,  $Q$  is the total amount of charge stored and  $V$  is the external voltage applied. The capacitance of a capacitor can vary in the response to applied voltage. In such case we can find the capacitance by taking differential of charge ( $Q$ ) with respect to the applied potential  $V$ .

$$C = \frac{d(Q)}{d(V)} \quad (1.2)$$

In case of an electrostatic capacitor having two conducting parallel plates with a surface area  $A$  and parted by an insulator with permittivity  $\epsilon$  and width  $d$ , the potential  $V$  can be demarcated as an integral of electric field  $\xi$  with respect the separation:

$$V = -\int_0^d \xi dx = \iint_0^d \frac{\rho}{\epsilon} dx = \int_0^d \frac{Q}{\epsilon A} dx = \frac{Qd}{\epsilon A} \quad (1.3)$$

Hence capacitance can be found as such

$$C = \frac{\epsilon A}{d} \quad (1.4)$$

It is quite evident from the above formula to assess the dependency of capacitance over permittivity of dielectric. The energy kept in a capacitor is set in following relation:

$$E = \frac{1}{2} CV^2 = \frac{Q^2}{2C} \quad (1.5)$$

Another important parameter of capacitor is its power density which is expressed in the relation below

$$P = \frac{\sigma E}{\sigma t} \quad (1.6)$$

Here  $\sigma t$  is the discharging time of a capacitor.

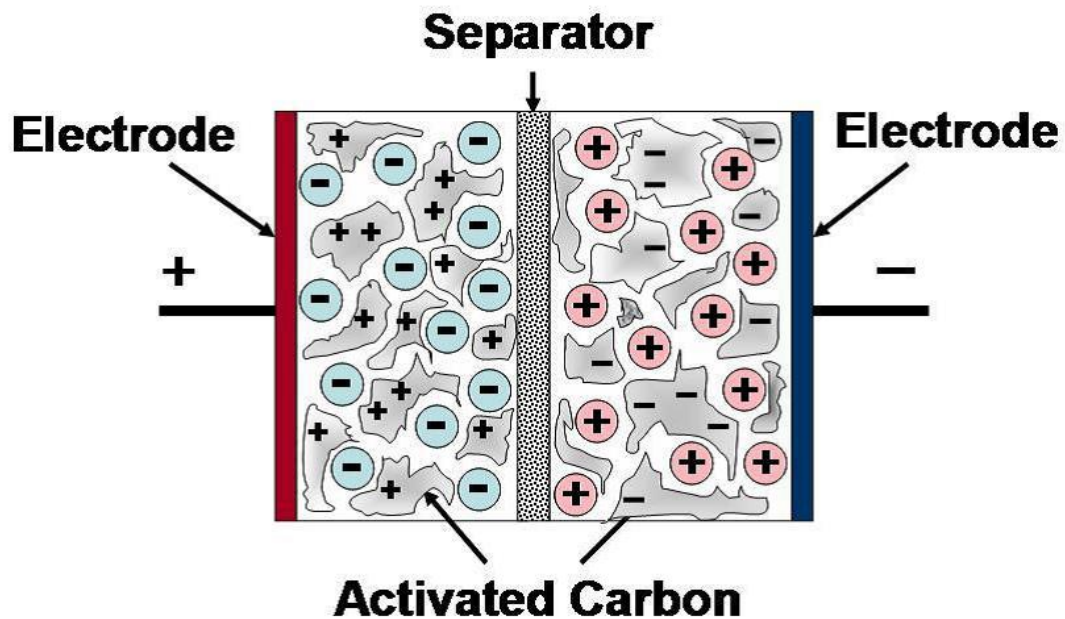


Figure 1.2 Illustration of supercapacitor [12]

### 1.1.2 Batteries

Till now electrochemical batteries have become the most crucial energy sources in consumer electronics and in many industrial applications. An electrochemical battery is a scheme that convert chemical energy into electrical energy in sequence of redox reactions. A standard battery consists of many cells and every cell consist of two probes attached by electrolyte containing charged species. Based upon the passage of ions inside a battery the polarity can be identified. Reduction at cathode and oxidation at anode are two set of redox reactions that power a battery. As the world is facing energy crises so to change the mode of energy production from burning fuel to some greener side and to shift the on-ground transportation to electric actuation. We require some sustainable energy alternatives. The electric vehicles has no internal combustion chamber with zero emissions to the environment and are driven by electrochemical battery.

In the near future of batteries used for consumer electronics, electric transportation and industrial application only Li-ion batteries show promise having considerable energy density and life cycle. At present the electric hybrid cars are available commercially (e.g. Toyota Prius) [13]. At present the Li-ion batteries has high acceptable energy density of 120-170 Wh/kg and adequate weight. Despite of the high energy density of

the Li-ion batteries and its substitutes the performance is limited by low power density and charge-discharge rates [14].

Schematic illustration of lithium ion battery is given below in figure 1.3

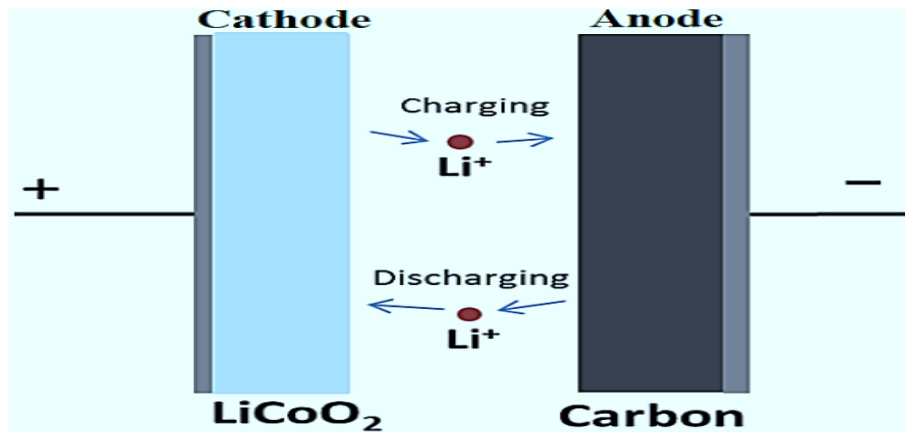


Figure 1.3 Schematic of Li-ion battery [14]

### 1.1.3 Fuel Cells

They are another sources of energy. Quite related to electrochemical batteries. These transform the chemical energy of gasoline to electricity. It is a device that combine oxygen and hydrogen to generate electricity having water and heat as waste. Its schematic illustration is given below.



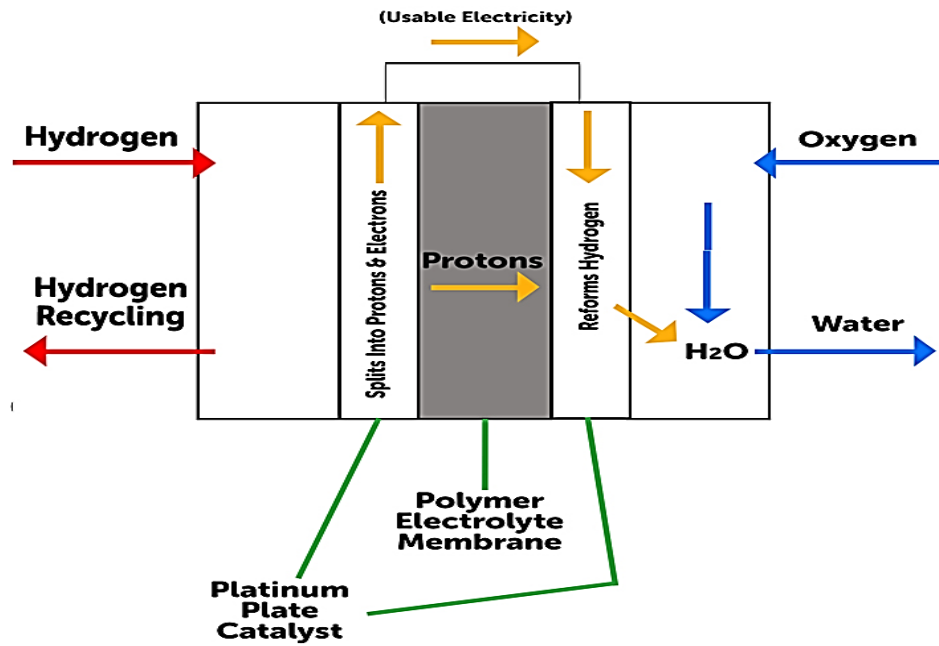


Figure 1.4 Schematic of fuel cell [15]

A fuel cell comprises of the following components.

- Cathode: reduction occurs at cathode
- Anode: Fuel oxidizes at anode release electrons
- Electrolyte: A chemical specie that is used for conduction of electron from one side to the other one inside fuel cell
- Catalyst: the electrode surfaces are catalyst coated
- Reformer: It extracts hydrogen from fuel

The traditional process occurring in a fuel cell for generating electrical energy is as follows.

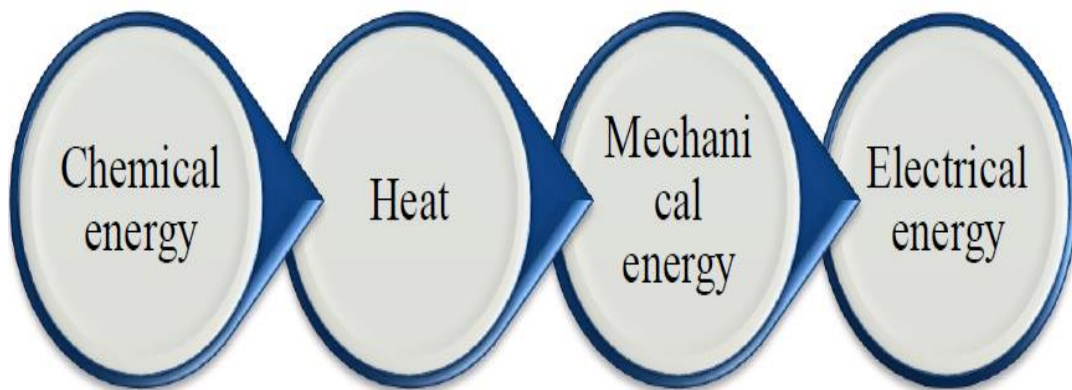


Figure 1.5 Energy flow diagram

Based upon the type of fuel and electrolyte fuel cells has the following types

- Molten Carbonate fuel cell
- Proton Exchange membrane fuel cell
- Phosphoric acid fuel cell
- Solid oxide fuel cells
- Alkali fuel cells

Compared to conventional thermo mechanical process, in fuel cells there is no combustion step as intermediate that is why it hold an efficiency up to 80%.

Limitation associated with fuel cells as alternative source of energy includes requirement of pure hydrogen, expensive catalyst such as platinum, high operating temperatures and corrosive electrolytes [15, 16].

### **1.3. Supercapacitors**

The limitations encountered in using fuel cells and electrochemical batteries as source of energy, such as low power output, expensive components and poor life cycle stability, a greater interest has been devoted to supercapacitors to compensate the lower power output attributes of batteries and fuel cells [17].

Schematic illustration of a general supercapacitor is presented is figure 1.5. A supercapacitor has a sort of sandwiched like geometry more likely of that of typical electrostatic capacitor and is composed of two electrodes which are highly porous in nature.

A supercapacitor principle is same as of ordinary electrostatic capacitors. When a power source is applied on the opposite terminals of electrode, charges begin to gather on the surface of the electrodes. The ionic species present in the electrolyte ooze out of the separator membrane as a result of law of attraction and enter the pores of the electrode material which in case of supercapacitors is excessively porous.

An important aspect of supercapacitor electrode materials is the design engineering. It should be designed in a way to prevent the unwanted recombining of ions. In order to get improved energy density and high capacitance, materials with high porosity and

greater surface area with least distance between the electrodes are favorable in supercapacitors [18].

The different types, information of each component of a supercapacitor, history and gradual development towards state of the supercapacitors will be discussed in chapter 2.

#### 1.4. Comparison of state of the art energy storage devices

A Ragone chart is presented below in figure 1.6 which is a normal way to assess the electrochemical performance of different state of the art storage devices [12, 19].

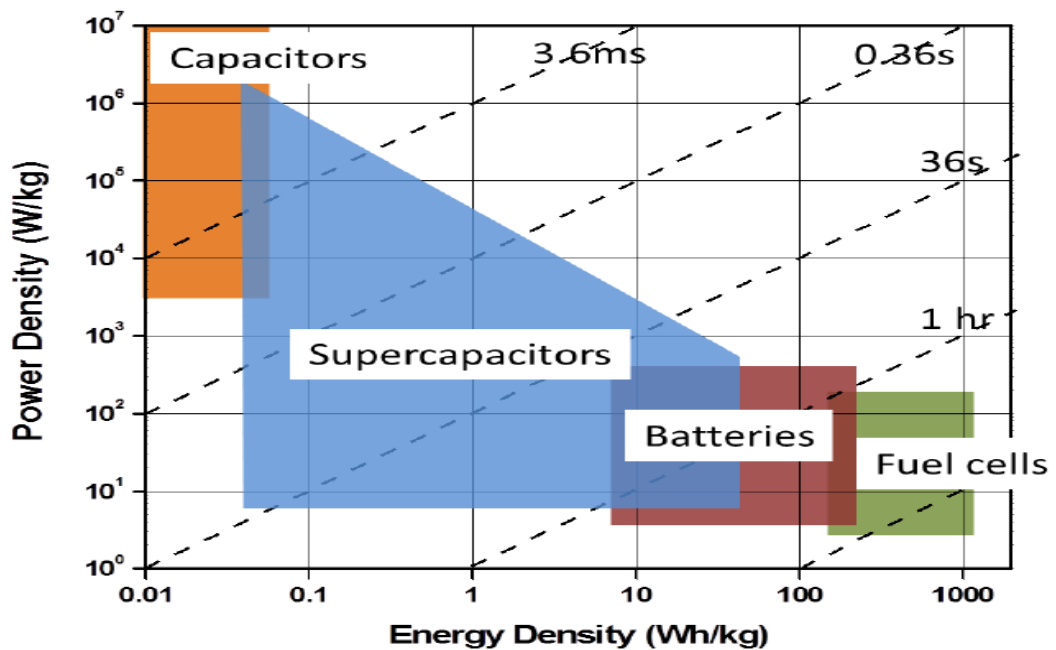


Figure 1.6 Electrochemical performance of different storage devices [12]

The time requisite for charging and discharging of a device is shown by dotted line. It is evident from the above figure that batteries among other energy storage materials can store a high extent of energy compared to conventional supercapacitors with poor power density. Also from the chart it is clear that conventional capacitors provide a high output related to other sources but are limited by poor energy density. Supercapacitors are accomplished of storing higher energy than traditional capacitors and also can provide much more high power density equated to batteries or fuel cells. The charge discharge time of supercapacitor is impressively lower as compared to batteries. Apart from the other advantages over other energy storage devices

supercapacitors exhibit a very prolonged life durability reason for which are physical storage mechanisms and not corrosive chemical interactions [20].

### 1.5. Super capacitor applications

Due to its significant fast charge discharge characteristics supercapacitors have become potential candidates in many applications where high power impulse is crucial. Figure 1.7 below shows some important applications of supercapacitors



Figure 1.7 Schematic showing applications of supercapacitor [13]

### 1.6. Research motivation

In mandate to stunned the limitations related with supercapacitors such as lower energy density, lower capacitive performances of ELDCs and poor life durability of pseudocapacitors improvement of the current formal of the art technologies is necessary. Research in the arena of materials science with aims of finding materials that can link the gap between supercapacitors and batteries is vital.

Investigations behind the reason for retarded life cycle of pseudocapacitors consisting of metal sulfide nano structures revealed that agglomeration of active electrode material is the cause for low performance [21].

A scalable hindrance of performance is also observed by the localization of charge transferal process to the surfaces of nano materials especially in case of inorganic materials [21].

The combination of binary transition metal sulfides with carbon material can be an adequate approach to design material that will have excellent pseudocapacitive and ELDCs performance [22].

## **1.7. Research objectives**

The goal of this work is the demonstration of efficient nano materials to meet with the challenges confronted in the field of supercapacitor research. Based on our findings the ultimate goals of this research are

- The exploitation of pseudocapacitance of transition metal sulfides and durability of materials of carbonaceous origin.
- Synthesis of binary transition metal sulfides nanostructures.
- Immobilization of binary metal sulfides nanostructures on the surface of MWCNT's.

## **1.8. Dissertation organization**

This thesis comprises of the following six sections as;

**Chapter 1** gives a brief insight of research work, motivation behind the selection of this area of research and objective statement of work.

**Chapter 2** covers the literature review regarding supercapacitor electrode materials, history of supercapacitor, gradual progress in the field of supercapacitor research, different types of supercapacitor and limitation regarding supercapacitors. This chapter also cover an adequate approach to address the drawbacks of supercapacitors.

**Chapter 3** presents a comprehensive review on experimentation technique utilized for binary metal sulfide nanostructures synthesis, in situ fabrication of binary metal sulfides and carbon nano tubes composite, characterization methods and testing methods used to estimate the act of nanocomposite.

**Chapter 4** the results gained from the synthesis procedure will be discussed. Also, the results from the different characterization techniques such as SEM and XRD will be debated. More over the electrochemical performance evaluated by electrochemical characterization such as CV and GCD will be addressed

**Chapter 5** gives the conclusion of the research work. It gives an insight of the objectives achieved.

## **Summary**

This chapter gives an introduction of energy storage devices that are used nowadays to store energy. A summary of the state of the art of these devices such as capacitors, fuel cells and batteries along with their working principles is given. Comparison of existing devices is done. Furthermore this chapter covers the research motivation behind selecting this specific topic. The goals of the current research work are also illustrated. In the last the organization of thesis is presented.

# Chapter N0. 2

## Literature Review

### 2.1. Emergence of Super capacitor

Innovation of the potential of charge storage over conductive surfaces came from the rubbing phenomenon of different materials, witnessed in early ages. The emergence of these kind of properties was not understood till the mid of eighteenth century. The understanding of electricity at molecular level started some 170 years ago, secondarily with research of Michel faraday, Millikan and J.J. Thomson. In connection to the early explorations of reasons associated with effects of static electricity, the advent of Leyden jar 1746 at Leyden in the Netherlands, the investigations of charge storage and separation mechanisms on the surface of jar with glass as separator were of Vitol importance in the field of science of electricity, electrochemical, electrical technologies and electronics. The device was referred as “Condenser” in the early works and it was attributed to Dean Kleist at Leyden and concurrently to Kamin, Pomerania. Later on the terminology for the condenser changed and took the term of “Capacitor” in many different embodiments and its potential in terms of charge storage was referred as “Capacitance” [18]. The very first patent awarded to Becker in the field of supercapacitor research dates back to the year 1957 [23]. Taking advantage of the high superficial area of carbon based materials as an electrode SOHIO established the first commercial energy storage device in 1969, using tetra alkyl- ammonium salt as an electrolyte [24]. Nippon Electric Company (NEC) come up with the first successful commercial electric double layer capacitor under the title “supercapacitor” in 1971. The internal resistance of these devices was high due to their low voltages, were primarily used for memory back up applications and many other consumer appliances. In the year 1978 the first gold based storage devices were marketed by Matsushita Electric Industrial (Panasonic, japan) with applications related to memory back up. The PRI (Pinnacle Research) in 1982 was the first in developing high power output electric double layer capacitor intended to be used in military application such as missile guidance and laser weaponry systems. A great extent of contribution was made to the field of supercapacitor research in the late 1970s and 80s by BE Convey and his

group exploiting ruthenium oxide based energy storage devices having least internal resistance and high capacitive performance [25]. In the field of hybrid electric automobiles supercapacitor attracted greater attention in the 90s. An intensive amount of work in regarding supercapacitor has been published and many patent have been granted [26].

US Department of Energy launched supercapacitor development long term initiatives in 1998-2003 and onwards which triggered studies in area of supercapacitor research. The commercial production of supercapacitor in the ongoing markets is based on highly porous carbonaceous materials exhibiting high surface area and transition metal oxide based systems. These commercial devices were used in many long term constant circuits, activators, in random access memory devices and telecommunication equipment.

## 2.2. Supercapacitors principle

A supercapacitor is an electrochemical device comprise of two conducting electrodes which are dipped in an electrolyte, partitioned by a divider and having current gatherers. The phenomenon of energy storage in supercapacitor is linked with the accumulation and distribution of collected charges on the surfaces of electrodes [19]. The capacitance  $C$ , In case of a planer capacitor having two plates as electrodes of area  $A$ , divided by distance  $d$ , in vacuum in a parallel configuration is given by equation 2.1.

$$C = \frac{A}{4\pi d} \quad (2.1)$$

When the separator between the electrodes is a dielectric medium of permittivity  $\epsilon$  the capacitance is presented by equation 2.2.

$$C = \frac{A\epsilon}{4\pi d} \quad (2.2)$$

Energy storage process in case of EDLC is the same, with the difference of charges accumulation in the electric double layer on the interface between conducting electrodes and electrolyte, quite than on the surface of electrodes. In case of charging the negative ions diffuse toward anode and the positive ions in the electrolyte diffuse toward the cathode. In such a case it develop two separate layers of energy storage [19].

The energy density  $W$ , of a supercapacitor is given by equation 2.3



$$W = \frac{1}{2} CV^2 \quad (2.3)$$

Here V is the potential and C is for capacitance.

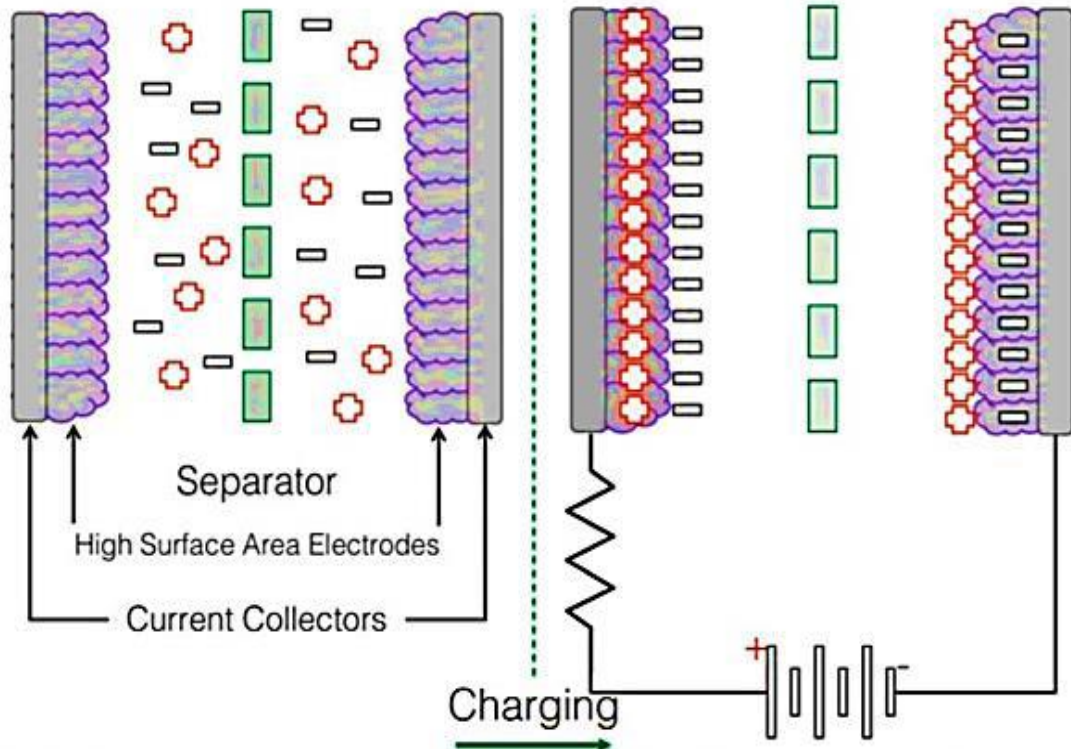


Figure 2.1 Schematic of supercapacitors function [19]

The energy storage mechanism in case of double layer capacitor does not involve any chemical reaction, a reason for improved cyclic performance. On the other hand capacitance contribution a result of chemical reactions concerning variations of oxidation state of ionic classes is also of great importance. This capacitance which results from faradic process is called pseudocapacitance.

### 2.3. An Electrochemical double layer

An electric double layer develops at the interface of be electrode and electrolyte, as a result of strong interaction of ionic species present in electrolyte. There exist a layer of charge on the metallic rod, resulting from lack or extra electrons. Furthermore there exist a layer of opposed charges in solution in the vicinity of electrode thus forming an array of opposite dipoles oriented across the metal solution interface which is called electric double layer. The capacitance resulting from electric double layer is somehow different from that of a traditional capacitor and is a function of applied voltage.

Various models such as Gouy-Chapman-Stern, Grahame and Helmholtz model are suggested to get an insight of the behavior of electrodes in electrolytic systems [27, 28]. Electric double layer can be visualized in the form of several different layers. The inner compact layer closer to the electrolyte is the inner Helmholtz, or Stern layer which consist of electrolyte molecules and in some cases certain adsorbed ionic species. Furthermore the compact layer can be branched into inner and outer Helmholtz layers. The inner Helmholtz layer is located at distance  $x_1$  from the electrical center of the absorbed species. The outer Helmholtz layer is present at distance  $x_2$ , which gives the least possible distance that the solvated species can reach the electrode surface or the starting region of diffusion layer.

The solvated ions are actually adsorbed nonspecifically, thus the contact between the solvated ions and charged electrodes involves only electrostatic forces and it does not depend on chemical nature of the ions. The ions which are adsorbed nonspecifically get distributed from the outer Helmholtz layer into the bulk of the solution owing to thermal agitation of medium and results in a three dimensional diffused layer, the thickness of which is dependent on the overall concentration of ionic species present in the medium. In an electric double layer the overall charge of the medium is a resultant of the total charge density of adsorbed species of interior layer and excess charge density of the diffused layer [29]. For this reason the electric double layer capacitance comprise of Helmholtz type capacitance denoted as  $C_H$  and diffuse layer capacitance given by  $C_{diff}$ , total capacitance of EDL is a combination of Helmholtz capacitance and diffuse region capacitance given below [23].

$$\frac{1}{C_{dl}} = \frac{1}{C_H} + \frac{1}{C_{diff}} \quad (2.4)$$

In these two layers the potential profile is very much different. The electric double layers capacitance is exaggerated by factors such the design of electrode and the nature of electrolyte used. A considerable volume of research work is published on graphitic carbon based electrodes [20, 30-33].

## 2.4. Pseudocapacitance

The origin of pseudocapacitance are the faradic process associated with chemical reactions involving change of oxidation states of the species of electrolyte. The pseudocapacitance observed in super capacitors is very much different in comparison with the EDLC. The mechanism of pseudocapacitance is similar to that of charging and discharging of a battery, the charges will transfer beyond the electric double layer.

Hence the pseudocapacitance can be considered by taking into consideration the amount of stored electric charge ( $\Delta q$ ) with respect to the variation of potential ( $\Delta V$ ) given in equation 2.5.

$$C = \partial (\Delta q) / \partial (\Delta V) \quad (2.5)$$

Generally, there is 1-5% contribution of pseudocapacitance in the capacitance of EDLC and it arose from the functional groups which are present on the active material. In the same trend there is almost 5-10% electric double layer capacitance observed in batteries. Pseudocapacitance results from either the electro sorption of H or metallic atoms and faradic processes which rely on the chemical attraction of electrode material to the active ionic species in the electrolyte. In one way the pseudocapacitance can exceptionally increase the capacitance of supercapacitors but it somehow limit the durability of supercapacitors by retarding their life cycle.

Material with superior pseudocapacitive performance which are extensively investigated include metallic oxides, hydroxide and sulfides of transition metals, for instance RuO<sub>2</sub>, MnO<sub>2</sub>, WO<sub>3</sub>, MoO<sub>3</sub>, Co<sub>3</sub>O<sub>4</sub>, NiO, IrO<sub>2</sub> and MnS, CuS, Ni<sub>3</sub>S<sub>2</sub>, ZnS and Go based Al<sub>2</sub>S<sub>3</sub> [40-44]. Electrically conducting polymers (ECPs) including polyaniline, polythiophene, polypyrrole and their derivatives have also delivered excellent pseudocapacitive performance with least stability [34].

## 2.5. Types of supercapacitors

Based on chemical configuration, different categories of supercapacitor anode materials which are considered conclusively contain transition metal oxides and sulfides like as MoO<sub>3</sub>, RuO<sub>2</sub>, MnO<sub>2</sub>, WO<sub>3</sub>, Co<sub>3</sub>O<sub>4</sub>, V<sub>2</sub>O<sub>5</sub>, Fe<sub>2</sub>O<sub>3</sub>, SnO<sub>2</sub>, NiO and IrO<sub>2</sub> as well as MnS, CuS, Ni<sub>3</sub>S<sub>2</sub>, ZnS and Go based Al<sub>2</sub>S<sub>3</sub> [35-44]. Electrically conductive polymers (ECPs) used in capacitors include polythiophene, polyaniline, polypyrrole their derivatives and composites with metal oxides [1, 45-50]. Other carbon based material used in ultracapacitors include activated carbon, carbons nanotubes (CNTs), carbon aerogels, graphene also composites of CNTs and graphene with metal oxides and metal sulfides [51-54].

## 2.6. ECPs based ultracapacitors

ECPs are electrically conductive due the presence of conjugated systems that can transfer electron along the polymer's backbone. Due to their acceptable cost, high charge density and most important their faradic reversibility ECPs are extensively

investigated during the past two decades [55]. ECPs having excellent conductivity, high pseudocapacitance and ease of fabrication technique have paved the way towards flexible supercapacitors [55]. An important aspect regarding ECPs is their morphology which significantly affect all parameter owing to its acceptability as an electrode material. A handsome amount of work is available in the literature related to the morphological varieties of ECPs which include bulk powder, nanowalls, nanosheets and nanorods. Nanostructured ECPs having exceptionally high porosity and high surface area deliver good capacitive performances as a result of the existence of discrete attributes of passageways, active surface interactions and superior surface to volume ratio. The ongoing research in the exploration of efficient ECPs has demonstrated that one dimensional nanostructured ECPs can provide very high performance in comparison to its bulk counterpart [34, 56].

### **2.6.1 Polyaniline**

A profound pseudocapacitive behavior has been reported for Polyaniline (PANI) for its use as positive electrode material. The attributes that make PANI a potential candidate for supercapacitor application is its excellent doping characteristics and variable oxidation states [57-59]. In spite of the fact that emeraldine, which is the protonated structure of PANI is found to have lower performance, still the polymers in this area are highly investigated for their environmental durability and excellent doping capability [60]. The maximum theoretical doping concentration which can be achieved for PANI is about 0.5 with a window of 0.7 V, with a theoretical capacitance value of 2000 Fg<sup>-1</sup> [68]. A large number of reports have been published on PANI as electrode material with capacitance ranging from 30 to 3000 F/g, the variation in capacitance can be linked with factors such as doping levels, structural morphology and fabrications processes. Nanostructured polyaniline/sodium alginate composites was synthesized in bulk form by Li et al. with capacitance of 2093 Fg<sup>-1</sup> has been observed for electrically polymerized composites compared to the chemically polymerized PANI [45]. Using tritonx100 in combination with electrically polymerized PANI a capacitance of 2300 F<sup>-1</sup> was observed [8]. PANI composite with porous carbon showed a stable and high capacitance of 1600 Fg<sup>-1</sup> [61]. State of the art ordered and specifically aligned nanomaterials, including PANI nanoforms has caught considerable attention for supercapacitor applications [62-64]. Vertically aligned ordered arrays of PANI nanorods in a template assisted approach based on supramolecular block copolymer assemblies achieved a capacitance of 3407 F/g [64].

The template based approach of fabrications quite complex and not applicable in large scale production. Kim et al come up with a novel idea of flexible supercapacitor based on PANI nanofiber attached to gold in a binder PVDF system and it showed improved performance [63]. The current advancements in search of overcoming the stability issues associated with polymer base electrodes involved the incorporation of carbon nanostructures such graphene and CNTs, which had a positive impact on the overall performance of supercapacitor [51].

### **2.6.2 Polypyrrole based ultracapacitors**

Among the ECPs investigated for an electrode material in supercapacitors polypyrrole offered appreciable performance due to its acceptable cost of fabrication, high thermal stability, fast charge-discharge rate and excellent energy storage capacity [65-68]. The pseudocapacitive performance of the polypyrrole electrode materials rely on the synthesis approaches and area of electrode material. Doping of PPy is normally done with single and multiple charged ionic species [66]. Cross-linked PPy systems have been reported to exhibit exceptionally high capacitance owing to their improved porosity of the active electrode material. PPy densely grown on the surface of the supercapacitor's current collectors inhibit the capacitive performances by reducing the active surface area of that reduce the access of dopant to polymer backbone. Zeng et al. reported an oxidation polymerization approach for the synthesis of PPy/ carbon aerogels and its application as supercapacitor electrode material delivering a maximum specific capacitance of 433 F/g [66]. Srivastava et al. achieved a capacitance of 395 Fg<sup>-1</sup> in Toluene/Sulfonate doped PPy/Carbon systems in inorganic electrolytes. Electro polymerization approach is used commonly for the PPy growth on the surface current collectors [69, 70]. In 2012 numerous nanostructures of PPy grown on the surface of stainless steel were reported by Dubal et al. by electrochemical approach for application in supercapacitor [71]. Among the variety of nanostructures designed for use in supercapacitor the nanosheets of PPy had better performance attaining a specific capacitance of 586 Fg<sup>-1</sup>. The nanosheet design of PPy grown on suitable substrate can be the futuristic approach in the fabrication of flexible supercapacitors. Nafion doped PPy based highly stable electrodes were reported by Kim et al. [70]. A few years earlier an easy "soak and polymerization" technique was reported for the fabrication of paper coated PPy by Yuan et al. This approach is one of the common method for the bulk fabrication of flexible paper based electrode materials [72].

### 2.6.3 Polythiophene based Ultracapacitors

Polythiophene and its other products have both n-type and p-type characteristics. In common the PTh have low conductivity but they have excellent stability in both normal and humid environment. PTh based ECPs have generally low capacitance in comparison to PPy or PANI but their advantage over the ECPs is their broad potential window [50, 73]. This broad potential window is helpful in the construction of asymmetric ECPs based devices. Among the derivatives of PTh, Poly (3-methyl thiophene) (PMeT), Poly (3(4-fluorophenyl) thiophene) (PFPT), Poly (3,4-ethylenedioxythiophene) (PEDOT), Poly(ditheno,thiophene) (PDTT) have better performance as electrode materials in supercapacitor and reported value of specific capacitance from 70-200 F/g [73]. The environmental stability of (PEDOT) is a reason for its exploration as pseudocapacitive material in the recent year [74-76]. The potential of electrochemically polymerized (PEDOT) in inorganic electrolytes was reported by Liu et al. [77]. PMeT/C electrode in gel-polymer electrolytic system and its application in supercapacitor was reported by Samui et al [78]. Kearns et al. come up with the idea of incorporation of appropriate and efficient redox couples in traditional PTh base ECPs systems and found that it can successfully improve the energy of power density attributes of a pseudocapacitor [79]. In another work Kearns et al. demonstrated a low cost simple copolymerization method using PT based system and its electro co-polymerization with triaryl amines achieving an improved cyclic capacitance compared to pristine PTs system [78]. A novel class of dendritic poly (tris (thiophenylphenyl)amine) (PTTPA) polymers was reported in 2012 by Robert et al achieving a specific capacitance of  $950 \text{ Fg}^{-1}$  in electrolyte systems [78]. Osterholm et al. used films of (PEDOT) as a flexible electrode material in both inorganic and organic electrolytes [77]. Minford et al. synthesized ultrathin films of PT and improved the performance by almost 250%. Nanostructures of the Poly (3,4-ethylenedioxythiophene) through a vapor phase polymerization approach were fabricated by D'Arcy et al. and it achieved a specific capacitance of 175 F/g. The PT based ECPs systems show promise the development of futuristic ECPs based flexible ultracapacitors.

## **2.7. Carbon based composite electrode materials**

Many derivatives of carbon are now being used as carbon nanotubes, carbon aerogels, activated carbon, and graphene for electrode materials in supercapacitor. Composites nanostructures of carbon with other polymers, metal sulfides and metal oxides.

### **2.7.1 Carbon nanotubes as an electrode materials**

Carbon nanotubes an allotropic form of carbon having its dimensions in nano scale exhibit high mechanical strength and conductivity. Multi-walled and Single-walled carbon nanotubes both are intensively investigated as electrode materials for EDLCs. It has been stated that the presence of an ultrathin uneven layer on the surface of CNTs can significantly increase the charge accumulation mechanisms in EDLCs [80]. From the literature review of EDLCs based devices it is evident that these devices provides a favor of high pseudocapacitance but one disadvantage of these materials is their low mechanical stability leading to extensive volume change, constant shrinking and swelling as a result of ions insertion and release. The use of composites of ECPs with CNTs in order to meet the challenge of low mechanical stability was reported by many groups [25, 52, 81, 82]. Among the composite materials conjugated ECPs are attached to the surface of CNTs effectively through  $\pi$ - $\pi$  interaction. A lot of research has been reported in the production of Polymer/CNTs composites in thin film or nanostructures architecture by oxidative or insitu electro polymerization for application in supercapacitor. Gupta et al. reported the successful synthesis of SWCNTs/ PANI composites and attained specific capacitance of  $463 \text{ Fg}^{-1}$  [25]. Sivakumar et al effectively fabricated MWCNTs/ PANI composites attaining a high capacitance of  $606 \text{ Fg}^{-1}$  [52]. On vertically aligned CNTs Zhang et al. coated PANI and attained a high specific capacitance of  $1030 \text{ Fg}^{-1}$  [83]. PPy was deposited potentiostatically on the surface of MWCNTs by Hughes et al. and he attained as specific capacitance of  $2.55 \text{ F/cm}^2$ . Li et al. synthesized a novel CNTs/PPy based core-shell structure in the form of sponge and reported as a highly compressible electrode materials with capacitance value up to  $300 \text{ Fg}^{-1}$ . Fang et al. used a pulsed electrodeposition method with narrow discrete pulses, allowing the PPy monomers to enter effectively into the pores of carbon materials achieving an impressive homogeneity in the coatings of PPy on carbon substrates [84]. Well aligned PPy/CNTs films having excellent flexibility through electrochemical method were reported by Lin et al. these films exhibited  $180$  degree bent flexibility along with high specific capacitance [84].

### **2.7.2 Graphene based electrode materials**

Graphene has got tremendous popularity among the other forms of carbon, mostly widely used in energy related systems. The unique characteristics of graphene that makes it important include its one atom thick 2D structure, high mechanical strength, innate flexibility, high conductivity and very high surface area. In the last decade a lot of interest has been devoted to combining graphene with ECPs systems for the fabrication of flexible electrode material [85]. The 2D design of graphene favors the transportation of charged species and also has a great influence over the morphology of ECPs/graphene composites. In 2010 the First ECPs/graphene composite was reported, in which graphene was functionalized with vertically aligned PANI nanostructures by electrodeposition and a specific capacitance of  $550 \text{ Fg}^{-1}$  was achieved [86]. Zhou et al. has fabricated PPy/graphene oxide (GO) based films for supercapacitor application by co-electrodeposition approach where the GO acted as weak electrolyte and also an efficient charge balancing dopant. Flexible, homogenous PPy / graphene composite films were reported by Davies et al. via a pulsed electro polymerization approach [87]. Flexible membrane polypyrrole nanowire and reduced graphene oxide (PPy-RGO) through insitu reduction were reported by Zhang et al. an unequal device was made-up by (PPy-RGO) composite and a high aerial capacitance of ( $175 \text{ mF/cm}^2$ ) was attained with this configuration [81]. In a report published on the PANI and graphene hydrogel (Gh) PANI/Gh it was found that in the proper engineering of PANI nanostructures significantly influence the properties of the composite. The PANI content when increased in PANI /Gh composites the capacitance exceptionally condensed from 1738 to  $574 \text{ Fg}^{-1}$  [81].

### **2.7.3 Activated carbon**

Among the carbon based materials activated carbons are also found to be used extensively in supercapacitor application because of larger surface area, low cost and their good electric properties. Activated carbons are commonly made from the chemical and physical stimulation of carbonaceous matter such as wood, nutshell, coal etc. Physical stimulation means the usage of carbon matter at temperatures ranging from 750 to 1200 °C. Chemical stimulation is generally conceded out at low ranging from 410 to 710 °C. Based upon the stimulation approaches and carbon precursor, ACs exhibit different properties with huge surface area up to  $3000 \text{ m}^2/\text{g}$  [88-91]. ACs resulted from both chemical and physical stimulation exhibited wide pore size distribution with micro (less than 2 nm), meso (2-50nm) and macro-pores (above



50nm). Research conducted in the exploration of ACs based electrodes discovered the contrariety between the huge area and capacitance, by attaining a capacitance of less than 10 F/g for an area of 3000 cm<sup>2</sup>. These findings revealed that high porosity is one of the important but not sufficient parameter for performance of storage devices. It can assumed that all the available pores were not effectively utilized. So the overall performance depends upon the homogenous pore size distribution, pore structure and shape, surface specificity and electric conductivity. The presence of moisture and acidic functional sites over the surface of ACs can inhabit life durability of supercapacitors [92]. An impressive amount of research has been reported with focus on finding the relationship between nano porous configurations and its capacitive performance in different types of electrolytes. Normally the ACs offers high capacitance in liquid electrolytes (100-300 F/g) in comparison to organic electrolytes (around 150 F/g). The carbon surface wettability by electrolyte is also a reason closely related to relative performance [93]. An optimum pore size of 0.4 nm has been reported by Salitra et al. for EDLCs [94]. Beguin et al. reported an ideal pore size of 0.7 nm for inorganic and 0.8 nm for organic media. All these studies emphasized on the important role of the pores which are electrochemically made accessible to the charged species of electrolyte thus influencing the overall capacitive behavior of ACs. Exploiting carbide-derived-carbons (CDCs) Largeot et al found out the essential relationship between pore size and ion size and suggested that for efficient EDLCs the pore size should be in agreement with the ion size [92]. Apart from the ACs porous structure the surface functionalization is also an important parameter as it is closely related to the wettability of ACs surface by charge species of electrolytes [95]. ACs having high content of oxygen functional groups having least porosity has been synthesized via carbonization. These materials exhibited high performance having high energy density up to 10 Wh /kg in inorganic electrolytes. Organic electrolytes is generally used in commercial supercapacitor application. . Hollenkamp and Pandolfo has given a comprehensive review on ACs with its main focus on the different types of functional groups, presence of trace water and the disadvantages of organic electrolytes . Many other studies focused on the low durability of ACs based device due to active carbon surface.

ACs have been used in the commercial production of super capacitor electrode material. Although their applications as successful future supercapacitor electrode

material is hindered by the challenge of proper pore size engineering and appropriate surface functionalities.

## **2.8. Metal oxide based ultracapacitors**

Metal oxides (MO<sub>x</sub>) and their composites with other compounds are believed to be one of most capable class of electrode materials for future generation ultracapacitors [96-98]. The advantage of (MO<sub>x</sub>) based electrode materials in comparison with other carbon based materials is its pseudocapacitive behavior resulting from faradic chemical reactions. The charge storage mechanism in carbonaceous material is based charge storage confined to the active area of electrode. A significant challenge to (MO<sub>x</sub>) based electrode material includes the volume induced structural variation and excessive loss of capacity over prolonged charge-discharge cycles. Due to poor electrochemical durability (MO<sub>x</sub>) based electrode material are suffered by excessive capacity loss and short life cycle. On the other side ECPs and Carbon based materials have good life cycle stability and also additional advantage of flexible design along with good electric conductivity. Hence, convincing synergistic effect are expected to be observed while combining (MO<sub>x</sub>) with different polymeric and carbon nanostructures (CNs) based electrode systems. Combined at molecular level these (MO<sub>x</sub>) based composite system can serve as efficient flexible supercapacitor electrode material with improved performance compared to single component systems [98, 99]. Recently the research in the field of supercapacitor was focused on combining the attributes of (MO<sub>x</sub>), (CNs) and (ECPs) to meet with the contests of energy storage capacity and life cycle stability confronted by individual component used as electrode material. (MO<sub>x</sub>) element generally impart high specific capacitance owing to its fast faradic process based on redox reactions. The (MO<sub>x</sub>/CNs/ECPs) resultant composite does not simply exhibit properties which are a sum of the properties of individual elements, but is in actual sense a completely new supercapacitor electrode material with unique properties and surface functionalities. Many reports have been published regarding (ECPs/MO<sub>x</sub>) based composites in which Co<sub>3</sub>O<sub>4</sub>, Fe<sub>2</sub>O<sub>3</sub>, TiO<sub>2</sub>, MnO<sub>2</sub>, RuO<sub>2</sub>, WO<sub>3</sub> and SnO<sub>2</sub> served as the MO<sub>x</sub> component, PEDOTs, PPy, PANI and its derivatives as ECPs components [100, 101]. Zhang et al. demonstrated as template free based approach for the fabrication of a cone shaped well aligned nanostructures of PPy/RuO<sub>2</sub> reaching a specific capacitance of 302 Fg<sup>-1</sup> [100]. Among the other MO<sub>x</sub>, RuO<sub>2</sub> has been extensively investigated for its application in supercapacitor having one important

disadvantage of relatively high cost. Hence the exploration of other economically acceptable and highly redox (MOx) based electrode materials for commercial application of supercapacitors is crucial. Therefore various research reports were published emphasizing on finding low cost (MOx) alternatives for successful commercialization of supercapacitors. In an approach toward the fabrication of promising supercapacitor electrode material MnO<sub>2</sub> based binary phased hybrids with ECPs has been investigated [101]. A ternary nanostructured based system of (ECPs/CNTs/MOx) has been reported by Hou et al. attaining a specific capacitance of 427 Fg<sup>-1</sup> with good life cycle permanence [101]. A notable capacitance of 2223 F/g was reported by Zhou et al. for 3D CoO/PPy nanowire composite [102]. A novel core-shell PPy/CNTs/MnO<sub>2</sub> composited is reported by Li et al. as efficient electrode material with synergistic effect from MnO<sub>2</sub>, (PPy) and CNTs conductive framework [102]. A PPy/MnO<sub>2</sub> composite film deposited on carbon cloth was reported by Wang et al. for its application as efficient electrode material

### **2.8.1 Binary MOx based electrode materials**

Due to superior electronic as well as electrochemical performance over single component oxide, the binary oxides with formula (AB<sub>2</sub>O<sub>4</sub>) such as CuCo<sub>2</sub>O<sub>4</sub>, ZnMn<sub>2</sub>O<sub>4</sub>, MnCo<sub>2</sub>O<sub>4</sub>, and NiCo<sub>2</sub>O<sub>4</sub> have attracted considerable attention among the researchers [103-105]. Porous nanosheets of double hydroxides layered with nickel and cobalt reported by Hao Chen and team delivered exceptional capacitance of 2682 Fg<sup>-1</sup> at 3 A g<sup>-1</sup> [106]. Ultrathin nano scale sheets of novel NiCo<sub>2</sub>O<sub>4</sub> were synthesized by Xu and coworkers through a facile template assisted approach and it delivered capacitance of 1468 F g<sup>-1</sup> at 2 A g<sup>-1</sup> [107]. Nanorod hybrid of nickel cobalt hydroxide and MWCNTs showed acceptable capacitance and storage density of 502 F g<sup>-1</sup> and 69 W h Kg<sup>-1</sup> respectively [105]. A capacitance of 2080 F.g<sup>-1</sup> at 1 A.g<sup>-1</sup> was reported with MWCNTs and NiCo<sub>2</sub>S<sub>4</sub> hybrids synthesized via solvothermal process [106]. To take advantage of good stability of Co<sub>3</sub>V<sub>2</sub>O<sub>8</sub> and high capacitance of Ni<sub>2</sub>P nanocomposite Co<sub>3</sub>V<sub>2</sub>O<sub>8</sub>/Ni<sub>2</sub>P was synthesized via precipitation approach and the 1002.5 F g<sup>-1</sup> at 1 A g<sup>-1</sup> capacitance was reported recently [107]. Nevertheless, the capacities reported for binary oxides of nickel and cobalt are restricted by fewer active sites that result from the agglomeration of nanomaterial of active electrodes. The performance is affected greatly by the localization of charge transfer process to the surface of nanomaterials especially in case of inorganic materials [22].

## 2.9 Metal sulfides based ultracapacitors

Metal sulfides and their composites with other compounds are believed to be one most capable class of materials for electrode future generation ultracapacitors [44]. The advantage of metal sulfides based electrode materials in comparison with other carbon based materials is its pseudocapacitive behavior resulting from faradic chemical reactions. The charge storage mechanism in carbonaceous material is based charge storage confined to the active area of electrode. A significant challenge to metal sulfides based electrode material includes the volume induced structural variation and excessive loss of capacity over prolonged charge-discharge cycles. Due to poor electrochemical durability metal sulfides based electrode material are suffered by excessive capacity loss and short life cycle. On other side ECPs and Carbon based materials have good life cycle stability and also additional advantage of flexible design along with good electric conductivity. Hence, convincing synergistic effect are expected to be observed while combing metal sulfides with different polymeric and carbon nanostructures based electrode systems. Combined at molecular level these metal sulfides based composite system can serve as efficient flexible supercapacitor electrode material with improved performance compared to single component systems [44]. Recently the research in the field of supercapacitor was focused on combining the attributes of metal sulfide, carbon nanostructures and ECPs to meet with the contests of capacity to energy storage and life cycle stability confronted by individual component used as electrode material metal sulfide element generally impart high specific capacitance owing to its fast faradic process based on redox reactions. The metal sulfide/carbon nanostructures resultant composite does not simply exhibit properties which are a sum of the properties of individual elements, but is in actual sense a completely new supercapacitor electrode material with unique properties and surface functionalities.

Due to superior electronic as well as electrochemical performance metal sulfides have highly attracted the researchers. Many reports have been published showing the metal sulfides for higher capacitance and long life. R.B. Pujari have reported MnS microfiber on the stainless steel as the substrate,  $747 \text{ Fg}^{-1}$  specific capacitance at  $1 \text{ mAcm}^{-2}$  current density [40]. W.Xu have reported CuS nanosheets on the nickel foam as substrate which have  $713 \text{ Fg}^{-1}$  capacitance at  $1 \text{ Ag}^{-1}$  the current density [41]. M.S javed have reported ZnS on carbon textile as substrate showing of  $747 \text{ Fg}^{-1}$  capacitance at  $1 \text{ Ag}^{-1}$

of the current density [43]. NiCo<sub>2</sub>S<sub>4</sub>/Co(OH)<sub>2</sub> core-shell nanotube like structures in situ deposited on Ni foam have been reported by R.Li showing 1055 Fg<sup>-1</sup> of capacitance at the 2 mAcm<sup>-2</sup> of current density [108]. Z. Xing have reported Ni<sub>3</sub>S<sub>2</sub> coated ZnO array on Ni foam which have 1529 Fg<sup>-1</sup> capacitance at current density of 2Ag<sup>-1</sup> [42]. P.Wen have supercapacitor reported NiCo<sub>2</sub>S<sub>4</sub> nanocluster anchored with multi-wall carbon nanotubes hybrid on Ni foam showing high capacitance of 2080 Fg<sup>-1</sup> at the current density of 1Ag<sup>-1</sup> [109]. GO based Al<sub>2</sub>S<sub>3</sub> Nanorambutan on Ni Foam have been conveyed by M.Faisal Iqbal showing the capacitance of 2178 Fg<sup>-1</sup> at current density of 3mA g<sup>-1</sup> [44]. Nanostructured nickel-cobalt sulfide deposited on nickel foam as electrode material for supercapacitor with high capacitance have been reported by X.F. which shows the 2068 Fg<sup>-1</sup> capacitance at 5 mA cm<sup>-2</sup> current density [41].

## 2.9. Challenges

From the above section it is clear that carbon based materials such as CNTs, CC, Go, RGO), metal oxide based materials (Co<sub>3</sub>O<sub>4</sub>, Fe<sub>2</sub>O<sub>3</sub>, TiO<sub>2</sub>, MnO<sub>2</sub>, RuO<sub>2</sub>, WO<sub>3</sub>, SnO<sub>2</sub>, metal sulfides based materials (CuS, MnS, ZnS, Ni<sub>3</sub>S<sub>2</sub>, CoS, Al<sub>2</sub>S<sub>3</sub>, electrically conducting polymer based materials (PPy, PANI, PT) and their composites in binary or ternary form can pave the path toward future's flexible and commercially acceptable supercapacitors. Furthermore, research reports demonstrate that the methods of composite fabrication also influence the electrochemical properties of resultant composites. Although the metal sulfide and carbon nanostructures based electrode material have higher capacitance but their overall performance like power density, energy density and stability are far away from the practical deployment of these devices in industrialized applications. Generally most of the research work regarding supercapacitor is mainly focused on the exploitation electrode materials and not on the complete fabrication of supercapacitor cell, and influence of the material on performance in different type of device configurations. Thus to meet with the challenges in the field of supercapacitor research, complete supercapacitor cell fabrication, some latest characterizations of a device interfacial opposition should be taken in account. In the last it is crucial to devote considerable attention to define some industrial standard for the successful commercialization of super capacitors.

## 2.10. Current efforts and future advancement

The carbon nanostructures, electrically conducting polymers, metal sulfides based materials and their binary and ternary composite system can revolutionize the pace of progress in flexible high performance supercapacitors. Future of CNs, ECPs and MSs based materials show a great promise for the next generation flexible, low cost and light weight energy storage devices. These composite based energy storage device are thought to occupy a significant sum of market portion of the present Li-ion technology in the coming years. The unique features of the composite based supercapacitors include excellent conductivity, superior pseudocapacitance, improved flexibility and ease of fabrication. Based on these unique features the composite material based flexible supercapacitors can be incorporated on cloth which can be readily stretched and rolled up. Recent researches in the field of supercapacitor electrode materials were very impressive but still there remain certain challenges hindering their deployment in real world applications. Certain potential declarations have mainly focused on achieving the following goals.

- Combination of binary transition metal sulfides with carbon material an adequate approach to design material that will have excellent pseudocapacitive and ELDCs performance.
- Enhanced mechanical stability high flexible electrode materials.
- Upgraded cycle stability using combination of metal sulfides and carbon nanostructures.
- Adjustability of active nanostructures with high energy, power density characteristics and organic/inorganic electrolytic systems.
- Direct growth of active electrode materials on current collectors for minimizing the associated internal and interfacial resistance
- Dual asymmetric flexible capacitors based on both n-type and p-type composite materials.
- Stability of supercapacitor materials for electrode is one of the fundamental issue in the commercialization of supercapacitors. Developing electrode materials by making composites with CNs such CNTs, GO, RGO, CC is approach for the improvement of active electrode materials. Apart from the

electrode engineering aspects, the selection of proper active electrode materials and type of electrolyte also play key role in achieving optimal performance. It is well reported that the improvement of working potential window of electrode materials is an efficient way for the enhancement of both power and energy density of supercapacitor. It is quite clear from the above section of literature review regarding electrode materials for supercapacitor applications, there still exist various challenges in the market acceptance of supercapacitor electrode base energy storage devices, a profound progress of research developments is foreseen in the near future.

## **Summary**

The above chapter summarizes the historical perspective, emergence and mechanisms of energy storage in energy storage devices. It also covers the different types of a supercapacitor which remained in practice. An impressive explanation of the different types of electrode materials used in ultracapacitors is provided. The research progress in the use of MSs, MO<sub>x</sub> and CNs systems as active electrode materials is given. Also the attempts in developing hybrid electrode materials based on the combination of state of the art electrode materials MSs, CNs, MO<sub>x</sub>, and CC are discussed. The challenges associated with the different parameters of supercapacitors performance such energy and power density are addressed. The challenges of design engineering and possible appropriate approaches to overcome them are debated. The problems confronted in achieving long cycle life are disclosed. Furthermore the issues faced in the selection of proper electrolyte systems and their possible influence over the overall performance of supercapacitor are described. The exploitation of synergistic effect produced between combining materials of different are well illustrated. The hurdles which are limiting the successful commercialization of electrode materials are highlighted. Lastly the different appropriate approaches that can readily overcome the hindrance in market acceptance of supercapacitors are presented.

# Chapter No. 3

## Methodology

In this chapter we will discuss about methodology adopted for fabrication materials and other characterization methods that are used in this research work.

### 3.1 Methods and materials

The synthesis of  $\text{NiCo}_2\text{S}_4$  nanostructures and its composite with MWCNTs is done via hydrothermal synthesis method. Nickel nitrate hexahydrate and cobalt nitrate hexahydrate served as the metal M (OH) precursor. The complete flow chart of the synthesis process and its different characterizations is given below in figure 3.1.

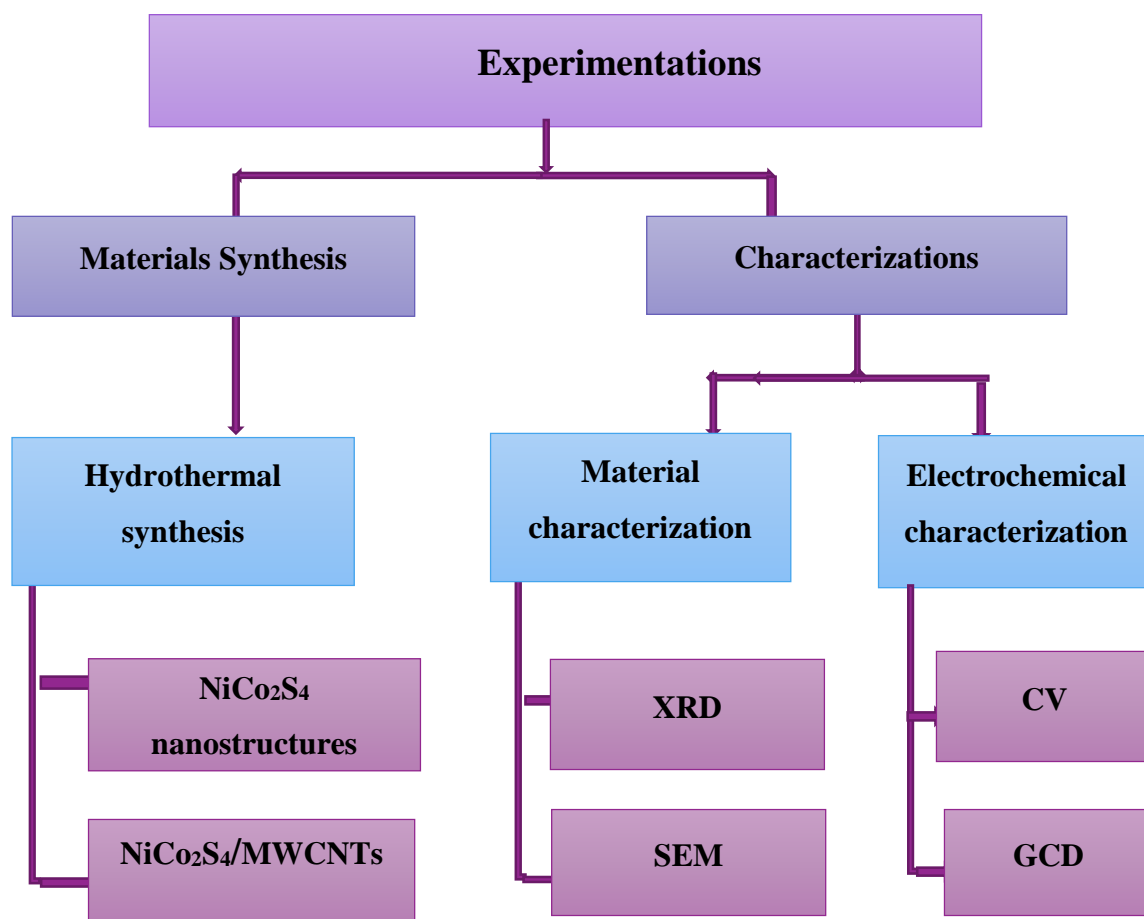


Figure 3.1 Flow chart of the synthesis process & characterizations



### 3.1.1 Synthesis of NiCo<sub>2</sub>S<sub>4</sub> nanostructures

Nanostructures of Nickel cobalt sulfide (NiCo<sub>2</sub>S<sub>4</sub>) are synthesized via hydrothermal method. Cobalt nitrate hexahydrate and nickel nitrate hexahydrate are used as metal precursor.

#### 3.1.1a Synthesis of metal hydroxide

In this synthesis, the metal hydroxide was initially prepared hydrothermal technique. Ni(NO<sub>3</sub>)<sub>2</sub>.6H<sub>2</sub>O (0.29 g), Co(NO<sub>3</sub>)<sub>2</sub>.6H<sub>2</sub>O (0.58), urea (0.6 g) and NH<sub>4</sub>F (0.3 g) were mixed in 60 mL of deionized water and magnetically stirred 30 minutes to form a rosy solution. Two pieces of Ni foam (2×1 cm) in an ultrasound bath were carefully washed with 3 M solution of HCl for 10 minutes to remove NiO layer, and then washed several times with ethanol and DI water. Then washed Ni foam was dehydrated in the electric oven. Above Ni foam and solution were then transferred into autoclave (100 mL) and kept at 120° C for 8 hours in muffle furnace. After the reaction for precursor deposition, autoclave was kept till its temperature comes down to room temperature. Then the sample of hydroxides /Ni foam were cleaned ultrasonically for 2 min in ethanol and water, and then dried overnight at 60°C. The glassware was first washed with distilled water and then with ethanol afterward dried in an oven. Schematic of different steps involved in synthesis is given below.

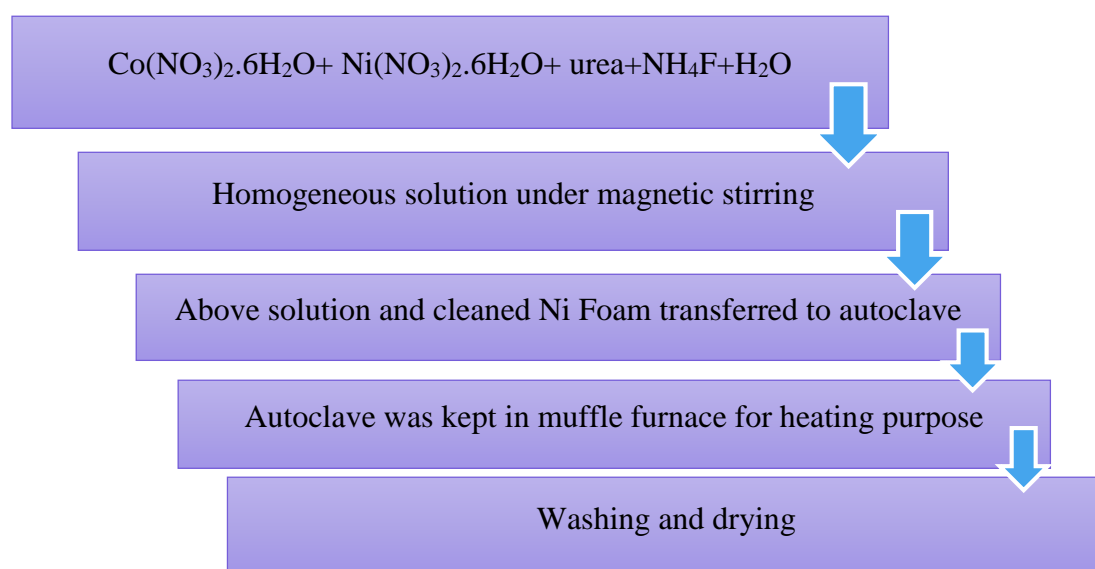


Figure 3.2. Schematic diagram of different synthesis steps of metalhydroxide nanostructures on Ni foam

A digital view of the binary metal hydroxides nanostructures deposited on the nickel foam is presented in Figure 3.3.

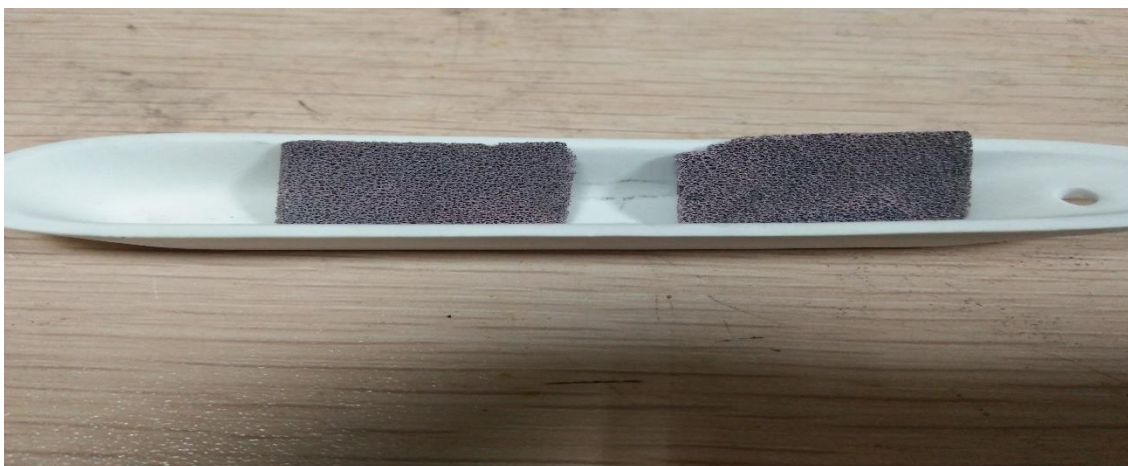


Figure 3.3. Metal hydroxide nanostructures deposited on the nickel foam

#### 3.1.1b Synthesis of nickel cobalt sulfides

In second step, 1.17 g  $\text{Na}_2\text{S}\cdot 9\text{H}_2\text{O}$  was taken and melted in 60 mL of deionized water under magnetic stirring. Then the Ni foam coated with precursor plus  $\text{Na}_2\text{S}\cdot 9\text{H}_2\text{O}$  solution were airtight in autoclave and retained at  $160^\circ\text{C}$  for 12 hours. The color of Ni foam changed to black. Then was washed with deionized water and ethanol for many times. Then dehydrated overnight in vacuum at  $60^\circ\text{C}$ .

Schematic of different steps involved in adopted synthesis route is given below.

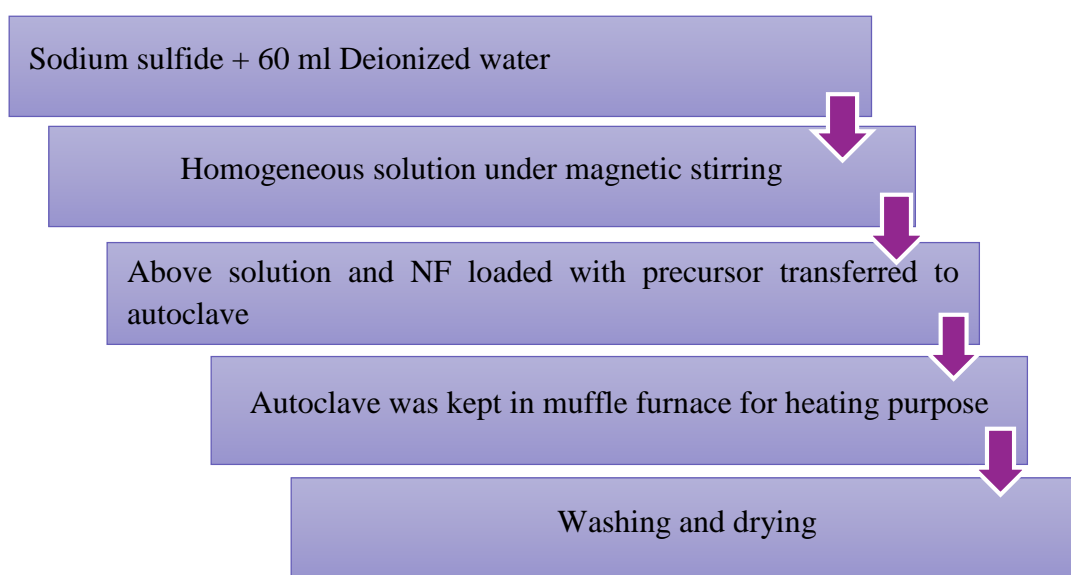


Figure 3.4 Schematic diagram of different synthesis steps of  $\text{NiCo}_2\text{Sulfide}$

### 3.1.2. Insitu decoration of MWCNTs and NiCo<sub>2</sub>S<sub>4</sub> nanostructures on Ni foam

In this present work, a simple hydrothermal method is used for the uniform decoration of MWCNTs with NiCo<sub>2</sub>S<sub>4</sub> nanostructures. In the first step the hydroxide / MWCNTs was primarily prepared via a hydrothermal method by adding an amount of 40 mg of MWCNTs and the remaining composition was kept same. For sulfide deposition, in second step 1.17 g of Na<sub>2</sub>S.9H<sub>2</sub>O were dissolved under magnetic stirring in 60 mL of deionized water and was repeated as discussed first.

A digital view of decoration of MWCNTs and NiCo<sub>2</sub>Sulfide nanostructures on the Ni foam is given below in figure 3.3.



Figure 3.5 Optical view of NiCo<sub>2</sub>S<sub>4</sub>/MWCNTs on Ni foam

In figure 3.6. Teflon-lined stainless-steel autoclave (100 mL) is shown, which is used for the hydrothermal method.



Figure 3.6 Teflon-lined stainless-steel autoclave



Figure 3.7 Muffle Furnace

## 3.2 Characterizations

The binary metal sulfide nanostructures and its composite with MWCNTs are successfully characterized through the following techniques.

### 3.2.1 Investigation of Morphology

Scanning electron microscopy is a straight forward mode to observe the apparent morphology and geometries nanomaterials. An ordinary microscope can only amplify up to 1000 times of a material because light is used in it for amplification having wavelength range of 400nm to 700 nm. Where, SEM uses electronic beam having wavelength much smaller than ordinary source of amplification having wavelength in the range of 400 to 700 nm, that makes able to achieve high quality resolution image of samples [110, 111]. Basic principle of SEM employs that when an electron beam strikes the surface of the sample, it interrelates with atoms of sample as a result of which results the back scattered, secondary electrons, characteristic X-rays are created that contain information relating to the topography, surface morphology of samples, and composition etc. SEM works in 3 operational modes namely primary, secondary and Tertiary mode.

- Primary: in this mode of operation SEM work with high resolution power of the order of about 1-5 nm range with secondary electron imaging
- Secondary: In secondary mode it linked with characteristic X-rays which are used for the identification of elemental composition of material sample via EDX technique.
- Tertiary: Tertiary mode produces back-scattered electronic images. It also traces the elemental composition of test sample.

The core restraint of SEM observation of sample material is the relatively small viewing field of SEM, which potentially increase the possibility that the section selected for the analysis may not be the sufficient representation of characteristics of the whole sample. More than one, for instance six different regions are observed and average information is achieved and considered in order to overcome this downside [110].

In the characterization of synthesized nanostructures and its nanocomposite, the detailed study of surface morphology of  $\text{NiCo}_2\text{S}_4$  nanostructures and also the confirmation of the attachment of MS NSs to the MWCNTs surface is deliberated by using SEM (Model: JEOL JSM-6490A).

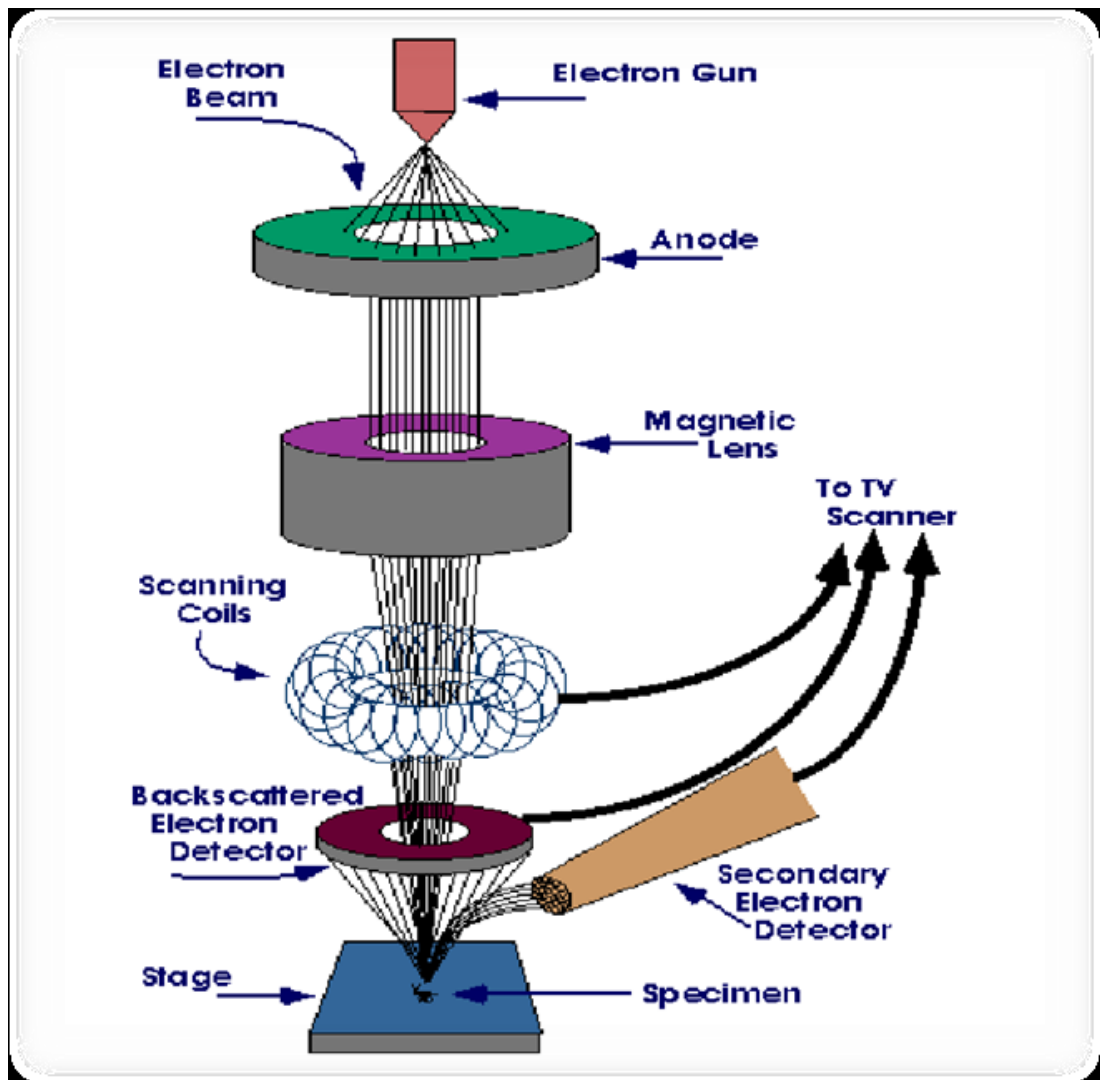


Figure 3.8 Schematic working of SEM [113]



Figure 3.9 Scanning Electron Microscopy (SEM) (Model: JEOL JSM-6490A)

### 3.2.2 Microstructure Characterization

X-ray diffraction (XRD) is an analytical and non-destructive technique revealing the information about the crystallographic structure of a material. Study of crystallographic structures is based on the phase identification and calculation of the dimensions of a unit cell. The importance of phase analysis is important because some time there exist an accountable dissimilarity, in capacitive performances of materials having same chemical composition, but different crystallographic planes for instance the single crystal systems have good performance in comparison with the



polycrystalline and amorphous materials [13, 112]. Furthermore it also provides information about the average crystallite size, crystal defects, structure type and preferred alignment of crystals along with other strain parameters. Working principal of XRD is based on the positive interference of monochromatic x-ray beams with target crystalline materials which undergo diffraction at lattice point and certain transmittance to reveal XRD spectrum. A schematic illustration of XRD is given below.

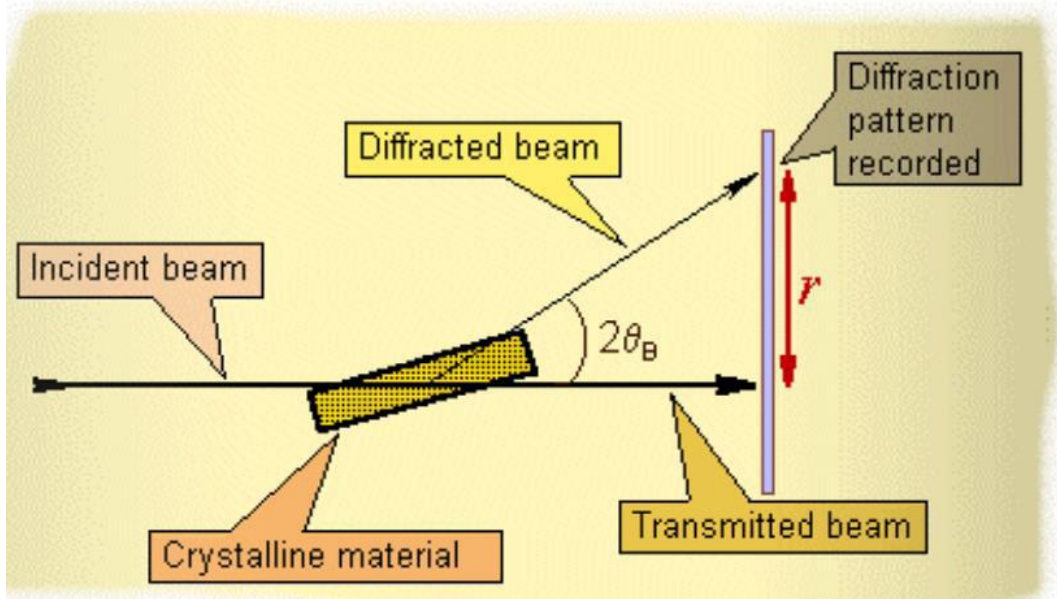


Figure 3.10 Schematic diagram of an XRD unit [115]

When an incident x-ray beam interact with a specimen (crystalline in nature) it follow the Bragg's law, as shown in figure. 3.9. While representing mathematically as:

$$2d \sin \theta = n\lambda \quad (3.1)$$

From above relation " $\lambda$ " is the x-ray's wavelength, " $n$ " is any integer, " $d$ " is the D-spacing between crystal (plane separation) and " $\theta$ " is the angle between occurrence beam and reflected beam.

While the crystallite size " $D$ " (nm) can be found by taking XRD major peaks using the equation given below:

$$D = \frac{0.94\lambda}{\beta \cos \theta} \quad (3.2)$$

Where “ $\beta$ ” is the full width half maximum, “ $\lambda$ ” is the wavelength of radiation having value (Cu  $K\alpha = 0.15406$  nm), and “ $\theta$ ” is diffracted angle.

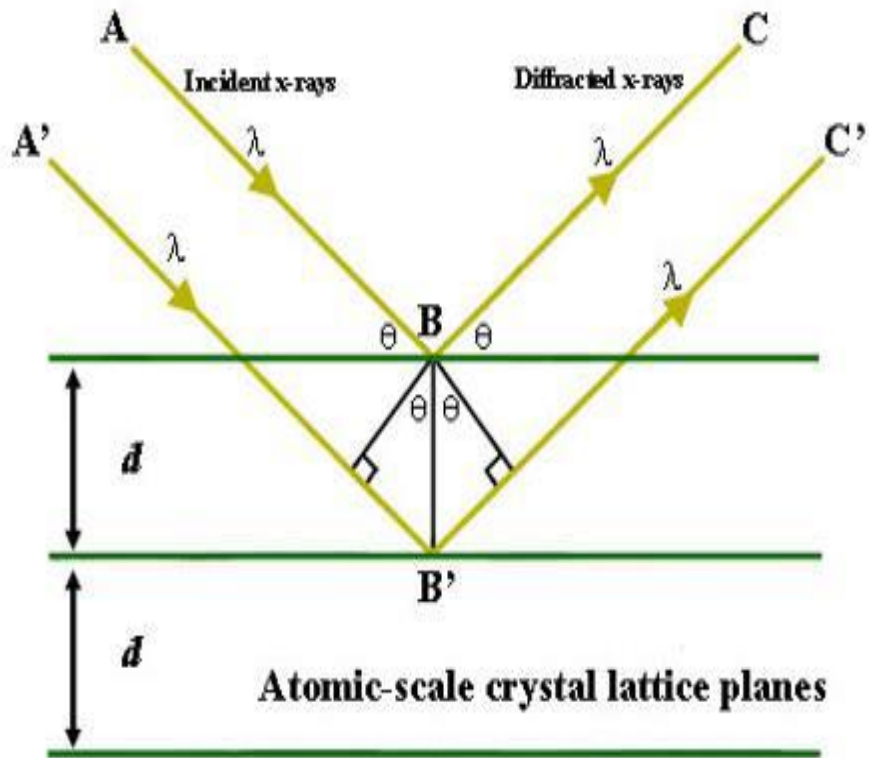


Figure 3.11 Bragg's Law, working Principle of XRD [116]

Theoretical density of the samples “ $\rho$ ” can also be calculated by given below:

$$\rho = \frac{MZ}{NV} \quad (3.3)$$

Here “ $M$ ” is molecular weight of material's ( $\text{g mol}^{-1}$ ), “ $N$ ” is Avogadro's, “ $Z$ ” represents the number of atoms per unit cell and “ $V$ ” ( $\text{\AA}^3$ ) is the volume of unit cell [112, 113].

Setup of XRD Spectrometer is shown below.



Figure 3.12 XRD Spectrometer (model D8-ADVANCE)

### **3.3 Electrochemical Properties**

#### **3.3.1 Cyclic Voltammetry**

The concept of CV was developed by (Shain and Nicholson) in the year 1964. In CV experiment the potential of an electrode is varied linearly from a point of no redox

reaction until the oxidation and reduction of the electrode species [43, 114]. Definition of some important electrochemical terms and basic features of cyclic voltamogram which is the result of a cyclic voltammetry experiment is given in the following section [115].

### 3.3.1.1 Definition of important electrochemical terms.

- **Electrode:** Generally an electric conductor made of a conducting plate such as a metal or graphite.
- **Electrolytic Solution:** Typically an aqueous solution of some dissolved inorganic salt.
- **Anode:** it is the electrode where an oxidation process happens.
- **Cathode:** At the cathode, reduction process takes place.
- **Charge:  $q$  [C]** Coluombic charge determined by integrating time-current values.
- **Current:  $i$  [A]** The flow of coloumbic charges measured in amperes.
- **Current Density:  $j$  [ $\text{Am}^{-2}$ ]** the amount of total current resulted divided by the surface area of electrode also sometimes termed as geometric current density.
- **Faradaic Current: ( $i_F$ ):** The type of current which is produced from redox reactions of active chemical species.
- **Peak Current:** Designated as  $i_p$  [A] it is usually the high value of current observed in CV experiment at the working electrode.
- **Peak Potential:** designated as  $E_p$  [V] is that potential associated with the working electrode at which the maximum current in a voltammetry experiment is obtained.
- **Scan Rate:** It is actually the voltage sweep rate per unit time in a cyclic voltammetry measurement.
  
- **Working Electrode (WE):** It is the electrode which contain our active material of interest and at its surface the desired electrochemical reaction is examined. The potential of this electrode is monitored closely in relation to the Reference electrode (RE) potential used in thee electrode system.

- **Reference Electrode (RE):** This electrode is usually a table and non polarizable electrode (Ag/AgCl, SCE etc.) and control the potential of the WE in a system of three electrodes.
- **Counter Electrode (CE):** The counter electrode (a Pt wire, or graphite rod) usually insures the chemical reaction occurring at WE by facilitating it in the reverse reaction.
- **Three-Electrode System:** An experimental arrangement composed of WE, CE, and RE used for electro analytical measurements.

### 3.3.1.2. Schematic illustration of CV system and principle mode of operation

In order to conduct cyclic voltammetry measurements on electro active materials of interest the following arrangement is necessary: The working electrode based on material of interest (WE), reference electrode (chosen according to material under investigation in WE), a counter electrode (CE) often called auxiliary electrode and an appropriate electrolyte that host the three electrode system. A schematic of three electrode system is given below.

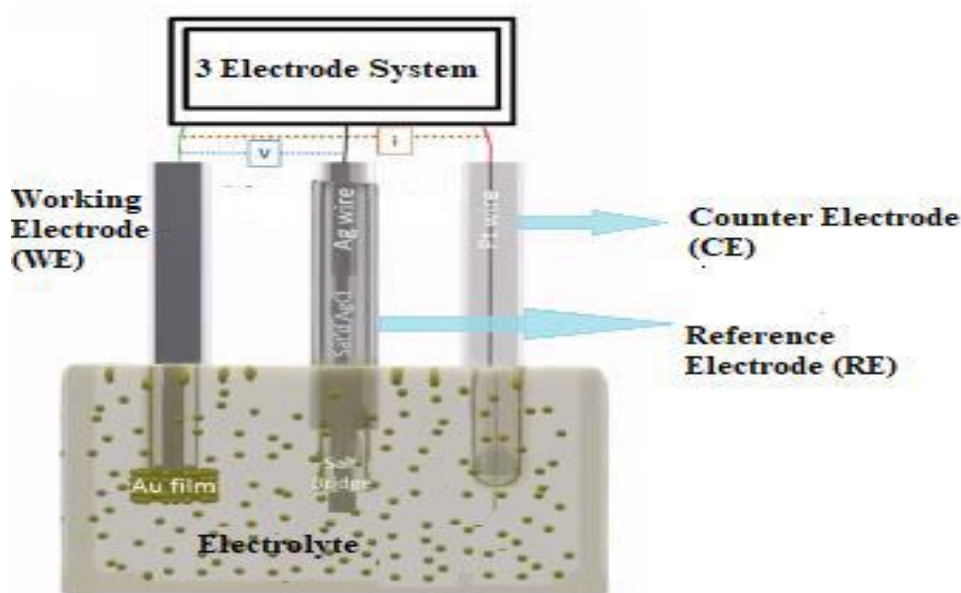


Figure 3.13 Representation of electrode system employed in CV [118]

Principles of a typical cyclic voltammetry curves generation is given the Figures 3.14 a, b and c below. In a cyclic voltammetry experiment a linear potential closely related to RE is applied to WE. At initial potential represented as  $E_1$  in the figure a CV scan start to generate, then it proceeds toward the final potential  $E_2$  and finally returns back

to potential  $E_1$ . The potential scan rate represented in ( $v$ ) is the variation of the applied potential as function of time ( $v$ )=  $dE/dt$ . Both the current flowing and the potential sweep rate can be deduced from a cyclic voltammetry curve as both are functions of time.

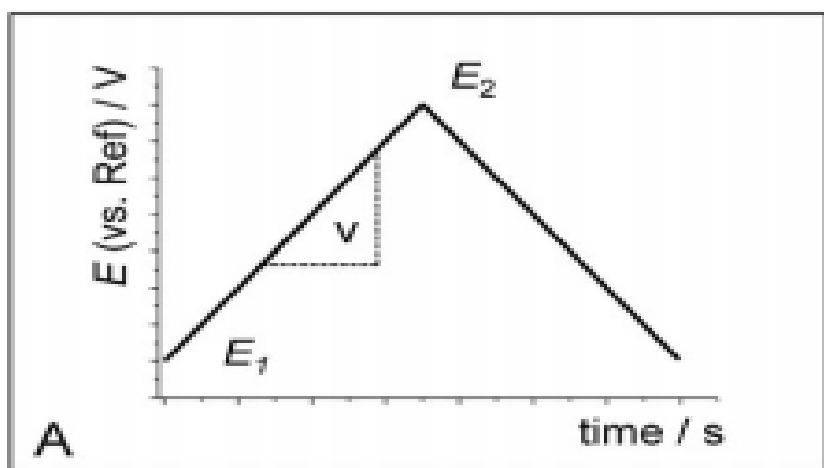


Figure 3.14 Cyclic voltammetry curve generation [118]

After applying potential to the W.E a CV scan begins at the initial potential  $E_1$  and proceed toward the final potential  $E_2$  and then returns back to the starting potential.

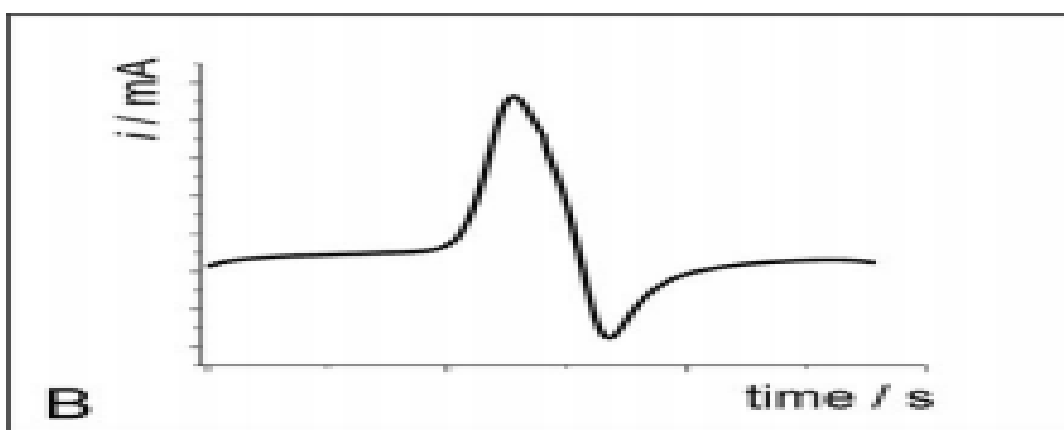


Figure 3.15 Current as a function of time [118]

Figure 3.15 shows the current produced as result of applied potential.

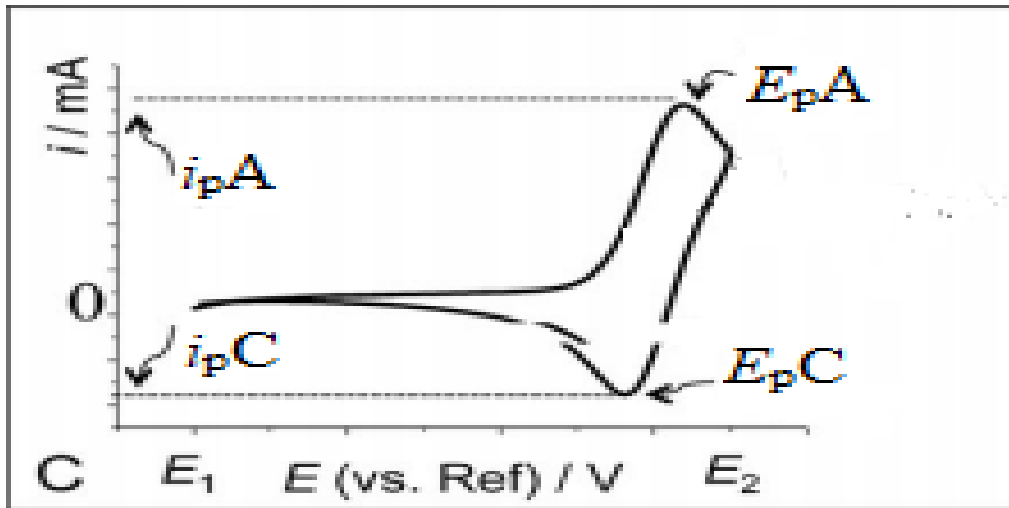


Figure 3.16 Typical cyclic voltamogram [118]

Fig 3.16. Shows current as a function of applied potential and this spectrum derived is called cyclic voltamogram. It also shows the maximum anodic current and potential labeled as  $i_{pA}$  and  $E_{pA}$ . The maximum cathodic current and potential is labeled as  $i_{pC}$  and  $E_{pC}$ .

### 3.3.2. Galvanostatic charge-discharge (GCD)

The GCD is a stable approach used for electrochemical evaluation of materials. The GCD method is quite different from cyclic voltammetry because in this procedure the current is organized and measurement of voltage is done. The GCD approach is one of the most widely used electrochemical techniques and it has the potential of extension from research laboratory to industrial scales. This technique is also sometimes termed as chronopotentiometry and it gives an insight of the following parameters such as

- Cyclability
- Capacitance
- Resistance

The principle of GCD is based on the use of a current pulse to the working electrode WE and the measurement of resulting voltage as purpose of time. The variation of voltage in a GCD test is given in the following equation 3.4.

$$V(t) = iR + \frac{t}{c}(V) \quad (3.4)$$

Here ( $t$ ) is the variable potential, as a role of time,  $iR$  is internal resistance,  $C$  is the capacitnce and  $i$  is the current. It is clear from equation 3.4 that capacitnce  $C$  can be easily calculated by using slope of the GCD curve.

In case of a pseudocapacitor the  $V(t)$  not varies linearly in a  $V(t)$  curve profile, so the capacitance can be considered by the integration of current over discharge time as given in equation 3.5

$$C = I \frac{\Delta t}{\Delta V} \quad (3.5)$$

Here  $I$  for current,  $\Delta t$  for discharge time and  $\Delta V$  for potential window.

All electrochemical measurement were recorded using a Bio Logic VSP workstation. Nickel foam on which the active electrode material was deposited, served as direct WE, KCl electrode served as RE and counter electrode of Platinum wire was used. 2 Molar potassium hydroxide (KOH) solution in deionized water was used as electrolyte [41].

The instrument used for the electrochemical measurements is given in the figure 3.17.



Figure 3.17 Schematic of Bio Logic VSP instrument used for electrochemical measurements.



## **Summary**

This part provides a broad review of the materials used in the current study along with the methodology adopted. Diagram illustration of the whole experimentation process is given. The binary metal sulfide nanostructures were synthesized via hydrothermal method using the nitrate salts of respective metals. The fabrication of NiCo<sub>2</sub>S<sub>4</sub>/MWCNTs nanocomposite is discussed in detail, which is done by an insitu approach via hydrothermal method. Information of different steps involved in the fabrication process is presented. The different approaches for the characterization of nanomaterials such XRD, SEM and their working principles are discussed. In the end the techniques employed for electrochemical characterizations such as CV and GCD along with their working principles are illustrated.

# CHAPTER No. 4

## Results & Discussion

### **4.1. Electrochemical performance of supercapacitors, its challenges and possible potential remedies.**

Literature review analysis of supercapacitors electrochemical performance revealed that although the pseudocapacitance of metal sulfides based electrode material is very high but a significant challenge these materials includes the volume induced structural variation and excessive loss of capacity over prolonged charge-discharge cycles. Due to poor electrochemical durability metal sulfide based electrode material are suffered by excessive capacity loss and short life cycle. On the other Carbon based materials have good life cyclability but are limited by low EDLCs performances. Consequently, convincing synergistic effect are expected to be observed while combing metal sulfides with different carbon nanostructures based electrode systems. Therefore, this research work was designed to exploit the pseudocapacitance of transition metal sulfides and durability of materials of carbonaceous origin in order to overcome the challenges faced in the field of supercapacitors.

In the first step of this work nanostructures of binary metal sulfide  $\text{NiCo}_2\text{S}_4$  were deposited at the surface of nickel foam by hydrothermal method. In the second step the  $\text{NiCo}_2\text{S}_4/\text{MWCNTs}$  nanocomposite was fabricated in an insitu hydrothermal approach. This chapter give an insight of the results obtained from the fabrication process and different characterization techniques used to evaluate the performance of the anode materials in supercapacitor uses.

### **4.2. Morphological analysis of nanostructures**

#### **4.2.1. Morphological analysis of $\text{NiCo}_2\text{S}_4$ NSs**

In order to insure the successful fabrication of  $\text{NiCo}_2\text{S}_4$  structures in the nano regime scanning electron microscopy (SEM) is carried out. The morphology was investigated

through SEM. The SEM micrographs of bare nickel foam and NiCo<sub>2</sub>S<sub>4</sub> loaded on nickel foam is given below in figure4.1.

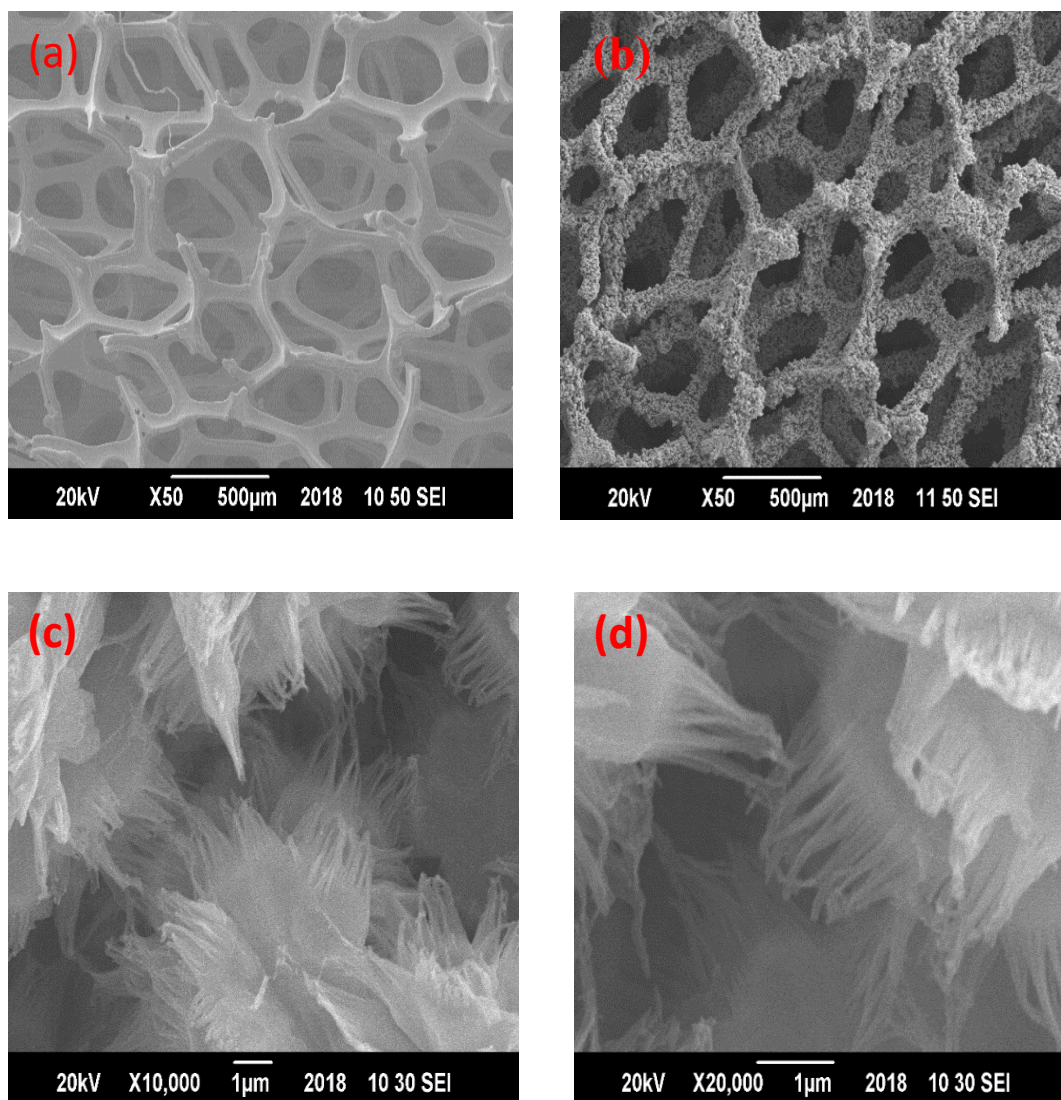


Figure 4.1 (a) SEM image of bare nickel foam (b) loaded with nanostructures (c), (d) shows NiCo<sub>2</sub>S<sub>4</sub> nanostructures.

#### 4.2.2. Morphological studies of NiCo<sub>2</sub>S<sub>4</sub>/MWCNTs composite

The morphology of the NiCo<sub>2</sub>S<sub>4</sub>/MWCNTs/Nickel foam composite is analyzed using SEM. The SEM images of nickel foam decorated with NiCo<sub>2</sub>S<sub>4</sub>/MWCNTs/Ni foam are given as following.

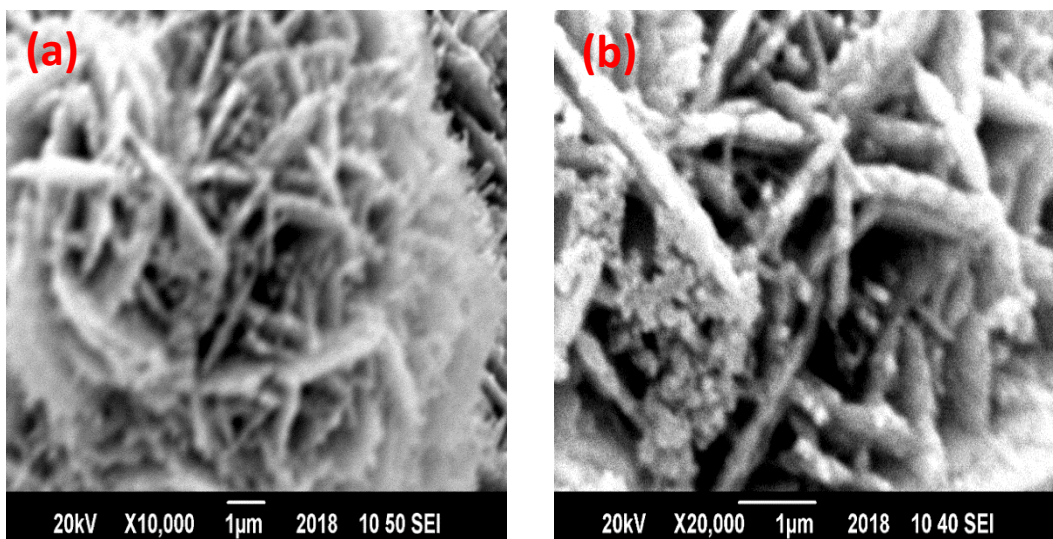


Figure 4.2 SEM images of nickel foam loaded with NiCo<sub>2</sub>S<sub>4</sub>/MWCNTs

From figure 4.1, image (a) shows the micrograph of bare nickel foam, (b), it can be realized that nickel foam is loaded with NiCo<sub>2</sub>S<sub>4</sub>. The SEM images from figure 4.1 c,d shows the nanostructures at different resolution. From c,d images it can be seen nanostructures have been grown the nickel foam.

In figure 4.2 SEM images clearly show that the NiCo<sub>2</sub>S<sub>4</sub>/MWCNTs composite has been placed on the nickel foam. The above SEM micrographs clearly shows the presence of nanostructure on MWCNTs anchored with the nickel foam. Nano particles in the beads are attached to the MWCNTs along different regions of SEM micrographs. These results are evident that MWCNTs are successfully decorated on nickel foam using the adopted method of fabrication. The goal of successful immobilization of nanostructures of binary transition metal sulfide has been achieved as depicted in SEM micrographs.

### 4.3. Phase and structural analysis

The XRD patterns of NiCo<sub>2</sub>S<sub>4</sub>, NiCo<sub>2</sub>S<sub>4</sub>/MWCNTs and bare Ni foam are given below.

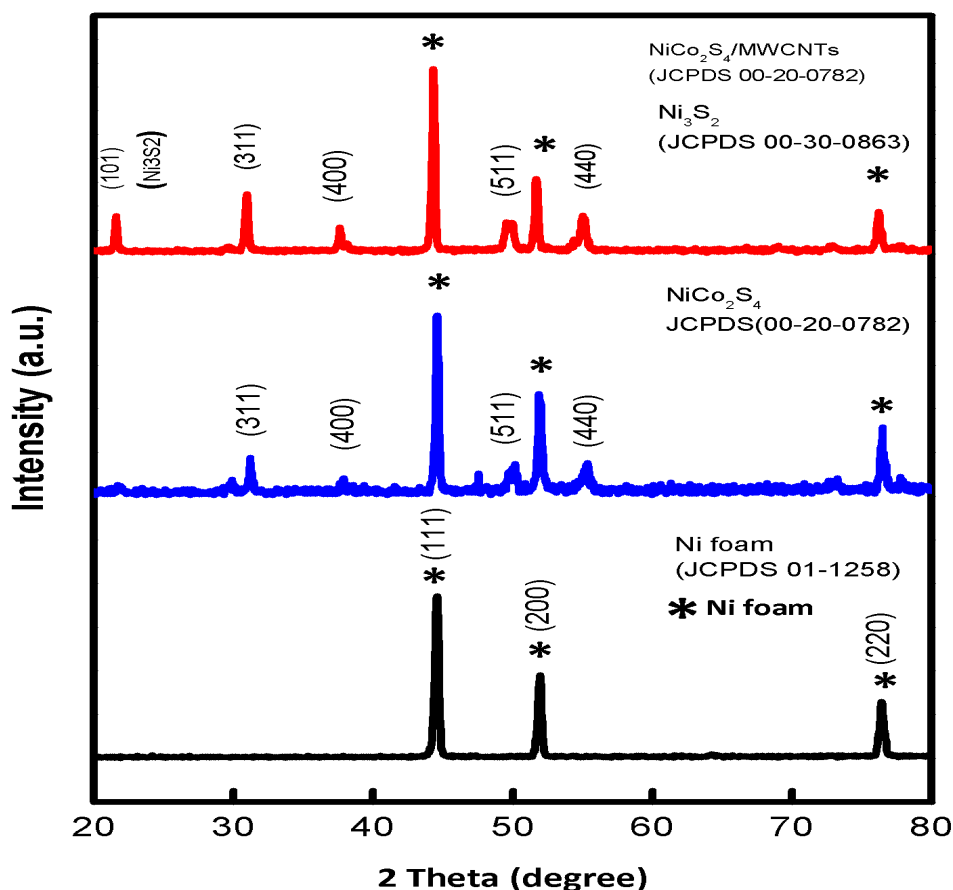


Figure 4.3 XRD patterns of NiCo<sub>2</sub>S<sub>4</sub>, NiCo<sub>2</sub>S<sub>4</sub>/MWCNTs and bare Ni foam

The XRD pattern of bare nickel foam shows the presence of nickel in a cubic structure typical of the nickel in accordance with JCPDF Card no's 00-001-1258. The highest reflection is shown for the nickel peak present at  $2\theta=44.370^\circ$ . Furthermore the peaks observed at  $51.596^\circ$  and  $76.084^\circ$  correspond to crystallographic planes (2 0 0) and (2 2 0) of nickel.

The figure endorses the formation of homogeneous cubic structure of NiCo<sub>2</sub>S<sub>4</sub> in complete agreement with PDF Card no. 00-20-0782. There are no impurity peaks detected in the pattern of NiCo<sub>2</sub>S<sub>4</sub>. The maximum noticeable reflection of the NiCo<sub>2</sub>S<sub>4</sub> is observed along the crystal plane (3 1 1) at  $2\theta=31.589^\circ$ . The other peaks observed at 38.320, 50.464 and 55.32 corresponds to the planes (4 0 0), (5 1 1) and (4 4 0) respectively. In case of the NiCo<sub>2</sub>S<sub>4</sub>/MWCNTs composites no peak shift was recorded. The XRD pattern of the composite shows an extra peak of (1 0 1) is observed at 21.76, which accounts for Ni<sub>3</sub>S<sub>2</sub> Rhombohedral phase (JCPDS 00-030-0863). Here no peak is observed for the MWCNTs due to low weight percentage and dumping effect. Moreover the peaks at 31.589, 38.320, 50.464 and 55.32 belong to the (3 1 1), (4 0 0),

(5 1 1) and (4 4 0) planes of cubic crystal structure. The XRD analysis of our materials confirms the successful fabrication of binary metal sulfide's cubic structure.

#### **4.4. Electrochemical studies of NiCo<sub>2</sub>S<sub>4</sub> and NiCo<sub>2</sub>S<sub>4</sub>/MWCNTs composite**

The electrochemical analysis of NiCo<sub>2</sub>S<sub>4</sub> and its composite with MWCNTs are carried out by three electrode system. The 2 molar solution of potassium hydroxide is used for electrolyte in this study. The nickel foam loaded with NiCo<sub>2</sub>S<sub>4</sub> and NiCo<sub>2</sub>S<sub>4</sub>/MWCNTs NSs is used as direct working electrode. The nickel foam 1×1 cm piece was connected with a wire by soldering and dipped in the electrolyte for electrochemical measurements. Ag/AgCl used for RE in this study. For counter electrode platinum wire is used. The electrochemical measurements executed include CV and GCD test.

Bio Logic VSP instrument is used in this study to explore electrochemical properties.

##### **4.4.1. Cyclic voltammetry of binary metal sulfide and its nanocomposite**

The electrochemical responses of the synthesized materials were performed by CV in 2 molar solution of KOH in the potential window of (0.0 -0.6 V). The active material deposited on nickel foam was used as direct electrode. The cyclic voltamograms of the NiCo<sub>2</sub>S<sub>4</sub> NSs and its nanocomposite are given in figures 4.8 to 4.11 at a potential ranging from 5 to 50 mVs<sup>-1</sup>. The oxidation and reduction peaks in the CV curves are due to the redox reactions of Co<sup>3+</sup>/Co<sup>4+</sup> as well as Co<sup>2+</sup>/Co<sup>3+</sup> and Ni<sup>2+</sup>/Ni<sup>3+</sup> conversions based on Eqs. (4.1) and (4.2) as given [41, 109, 116].



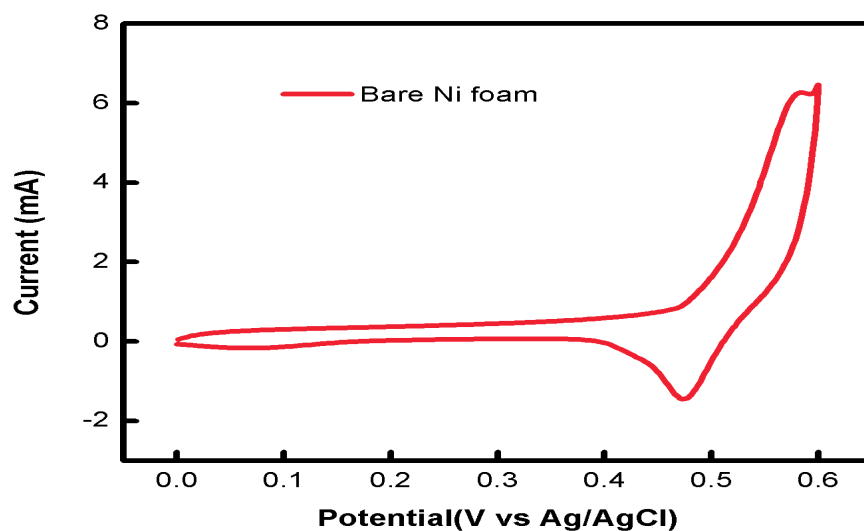


Figure 4.4 Cyclic voltamogram curve of bare nickel foam.

The above figure shows the CV curve for bare nickel foam electrode in a window of 0.00 to 0.6. From CV curve it is obvious that there happens a chemical reactions in case of the bare electrodes as the shape of the curve shows a redox peak in the region 0.56 and 0.48 of the curve. The max anodic current for bare Ni foam is almost around 6.2 mA at of  $20 \text{ mV}^{-1}$ , proposing the good electrochemical behavior of Ni foam.

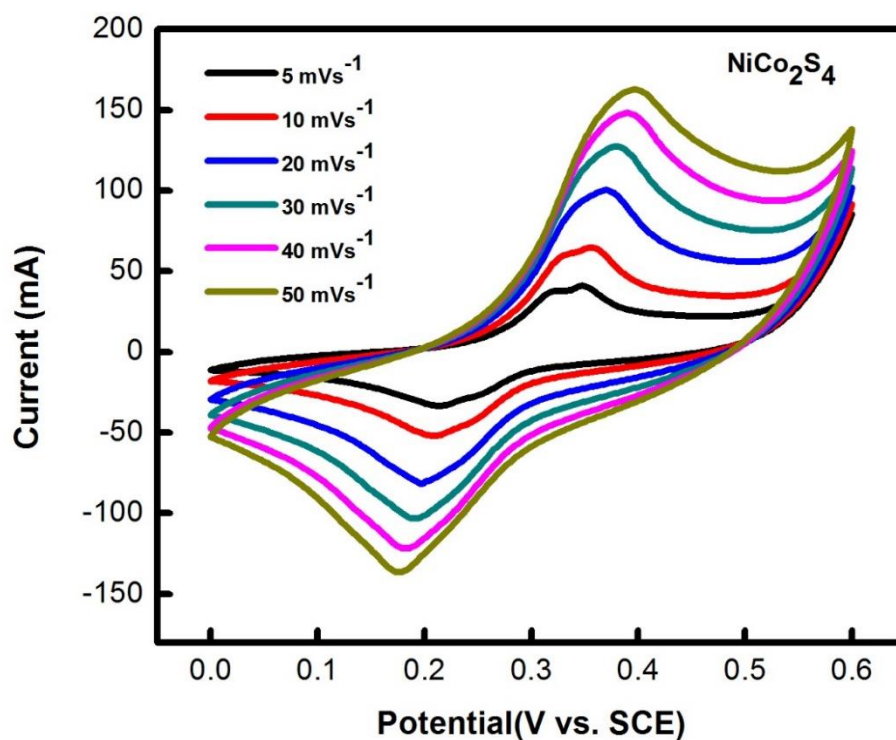


Figure 4.5 CV curves of  $\text{NiCo}_2\text{S}_4$  at different scan rates

Cyclic voltammetry scans done at scan rate of 50, 40, 30, 20, 10 and 5 mVs<sup>-1</sup>. Almost, all the curves are in the same trend with no noticeable variation in shape. The curve at 5 mVs<sup>-1</sup> has the lowest area and peak current while the curve at 50 mVs<sup>-1</sup> has the highest redox potentials. Furthermore, it can be understood from CV curves that a linear trend exist among the anodic current and scan rate. The peak anodic current in the CVs behaved in an increasing pattern with increasing scan rate signifying the good capacitive behavior of material. Capacitance calculation as of CV curves is done by the equation.

$$C = \frac{dQ}{dV} = I \frac{dv}{dt} \quad (4.5)$$

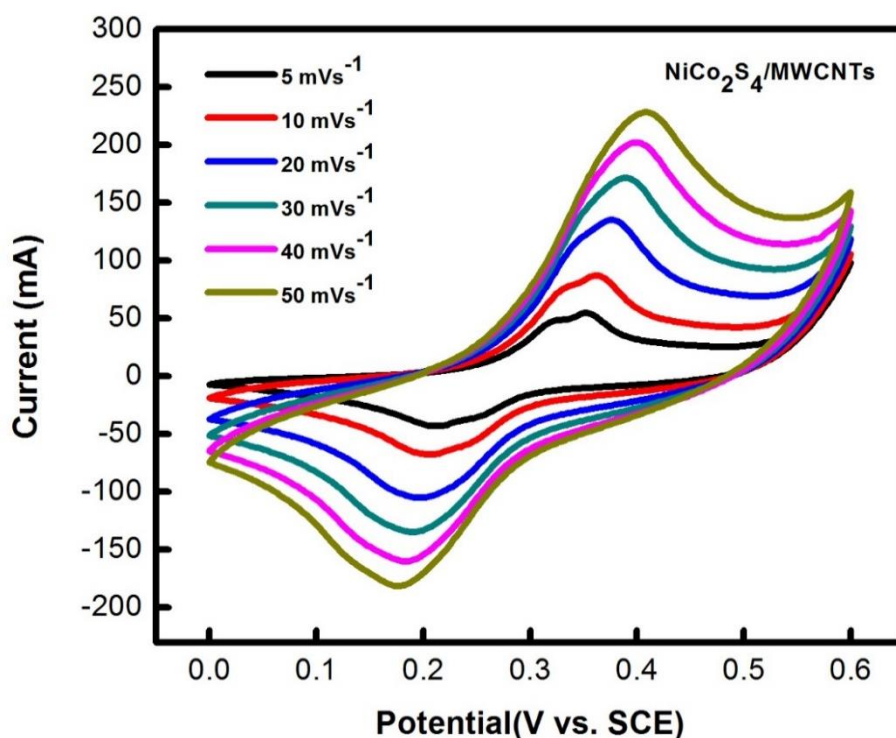


Figure 4.6 CV curves of the NiCo<sub>2</sub>S<sub>4</sub>/MWCNTs nanocomposite

The CV curves performed at dissimilar scan rates for NiCo<sub>2</sub>S<sub>4</sub>/MWCNTs are given above. It can be realized from the curves that a linear relation exist between the peak current and scan rate supporting the acceptable capacitive behavior. All the curves are in the same trend along the working potential window with no shifting of the corresponding redox peaks. More over the redox peaks sharpness has increased as the potential scan rate increases. At sweep rate of 50 most intensive redox peaks are recorded. The broader pair of oxidation-reduction peaks is observed for the curve at sweep rate of 50 mVs<sup>-1</sup>. The highest current density for NiCo<sub>2</sub>S<sub>4</sub>/MWCNTs



nanocomposite is recorded at a test rate of  $50 \text{ mVs}^{-1}$ . The CV scans at altered scan rates for both the  $\text{NiCo}_2\text{S}_4$  NSs and its nanocomposite with MWCNTs confirms the capacitive potential of both the materials. The comparative CV curves for both  $\text{NiCo}_2\text{S}_4$  and its composite with MWCNTs is given below in figure.

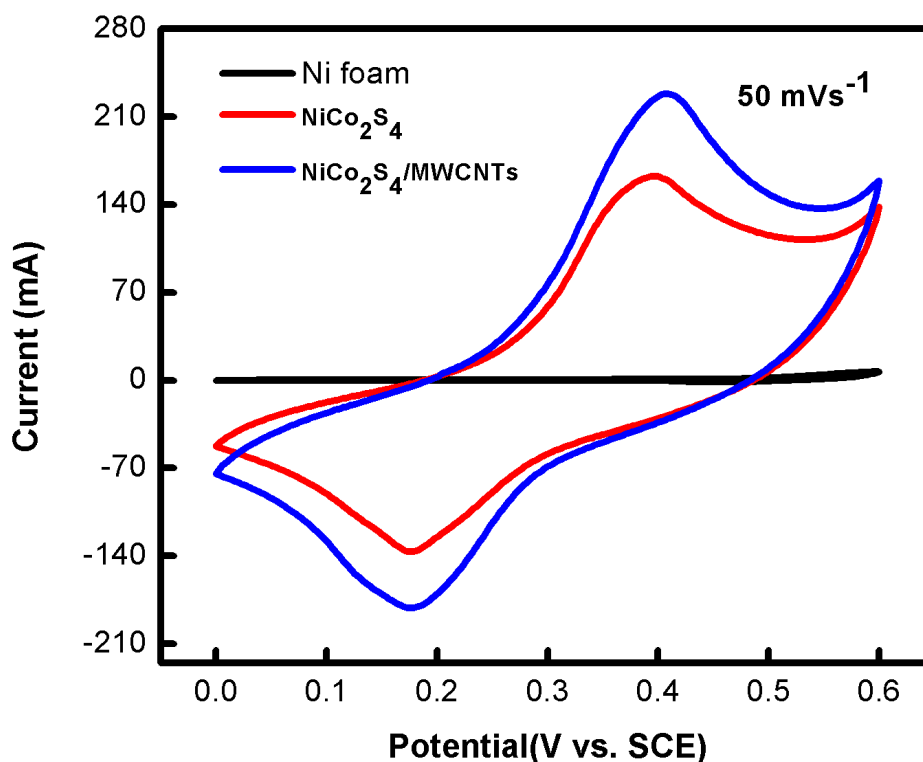


Figure 4.7 Cyclic voltammogram of  $\text{NiCo}_2\text{S}_4$  and  $\text{NiCo}_2\text{S}_4/\text{MWCNTs}$ .

Cyclic voltammetry for the NSs of  $\text{NiCo}_2\text{S}_4$  and  $\text{NiCo}_2\text{S}_4/\text{MWCNTs}$  nanocomposite performed in working window of (0.0 to 0.6 V) is given in above figure 4.7. In the CV curve of the nanocomposite sharp high intensity oxidation and reduction peaks are evident at 0.4 and 0.19 V respectively suggesting the pseudocapacitive behavior of the material. In case of the only  $\text{NiCo}_2\text{S}_4$  the broader oxidation, reduction peaks are observed at 0.38 and 0.17 V respectively. From the CV consequences it can be assumed that the incorporation of carbon structure has shifted the redox peak potentials toward the positive side. Furthermore the relatively lower CV curve area in case of only  $\text{NiCo}_2\text{S}_4$  can be correlated to the lower electrochemical performance. High current density in case of the  $\text{NiCo}_2\text{S}_4$  composite can be credited to the synergistic effect produced between metal sulfide NSs and carbon material. In one way the EDLC property of MWCNTs influenced the overall performance of the resulting composite in positive manner. On the other hand, the presence of MWCNTs has triggered the faradic process responsible for pseudocapacitance of  $\text{NiCo}_2\text{S}_4$  moiety in the

nanocomposite by providing a highly conductive scaffold. The relatively high current density and much higher integrated CV area is the result of the exploitation of combined properties of transition metal sulfides and carbon. The relation of peak current with the potential sweep rate for both the material is given in figure. 4.8.

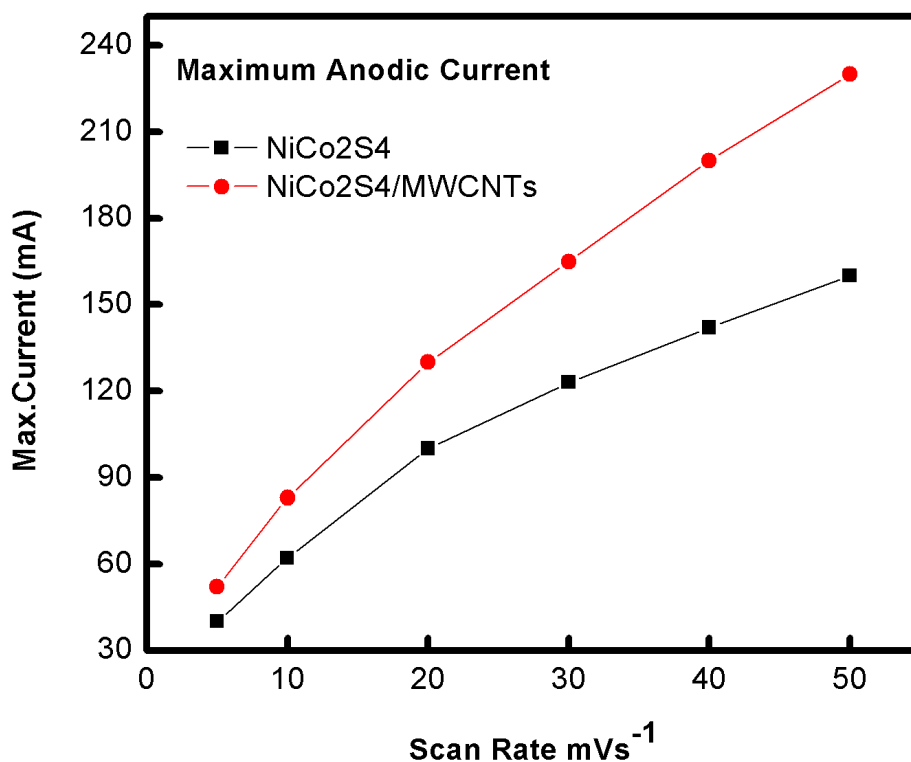


Figure 4.8 Max current vs potential scan rate for NiCo<sub>2</sub>S<sub>4</sub> and NiCo<sub>2</sub>S<sub>4</sub>/MWCNTs

The above figure shows a relation for both type of electrode materials between maximum anodic current and applied voltage sweep rate. The variation in the current with respect to the applied potential sweep follows a linear trend. As the scan rate has increased, the responsive anodic current also increased. The peak current in the case of NiCo<sub>2</sub>S<sub>4</sub> electrode material in positive direction for scan rate 5, 10, 20, 30, 40 and 50 mV/s is 40.05, 62.00, 100.08, 123.16, 142.00 and 160.05 mA respectively. The peak currents recorded for the composite at scan rate of 5, 10, 20, 30, 40 and 50 mV/s are 52.05, 82.80, 130.08, 165.10, 200.00 and 230.13 mA. The response of peak anodic currents to the voltage sweep rate for both the NiCo<sub>2</sub>S<sub>4</sub> NSs and NiCo<sub>2</sub>S<sub>4</sub>/MWCNTs nanocomposite confirms the capacitive behavior of the materials. Moreover the anodic current in case of NiCo<sub>2</sub>S<sub>4</sub>/MWCNTs is much higher as compared to the anodic current of NiCo<sub>2</sub>S<sub>4</sub> electrode material. This higher anodic current is also responsible for the higher capacitance in case of composite material.

#### 4.4.2. Galvanostatic charge discharge test

In order to examine the charge/discharge behavior of  $\text{NiCo}_2\text{S}_4$  nanostructures and  $\text{NiCo}_2\text{S}_4/\text{MWCNTs}$  nanocomposite GCD analysis was conducted at different current rates. The GCD analysis for both the materials are done in a three electrode assembly. The working potential window utilized for GCD analysis is 0 to 0.6. The GCD curves for the  $\text{NiCo}_2\text{S}_4$  NSs and its composite with MWCNTs at different current rates is give below.

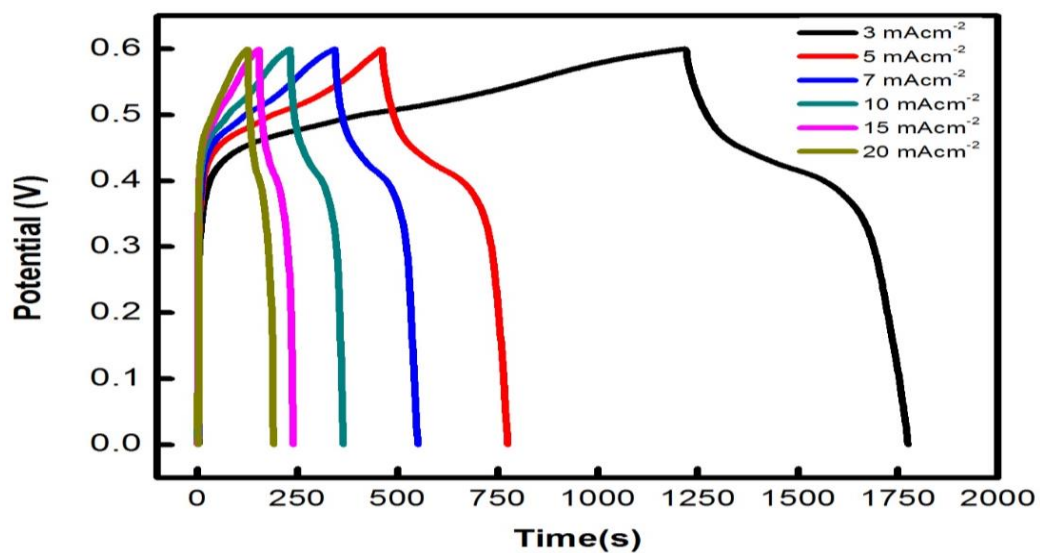


Figure 4.9 GCD curves for  $\text{NiCo}_2\text{S}_4/\text{Ni}$  foam

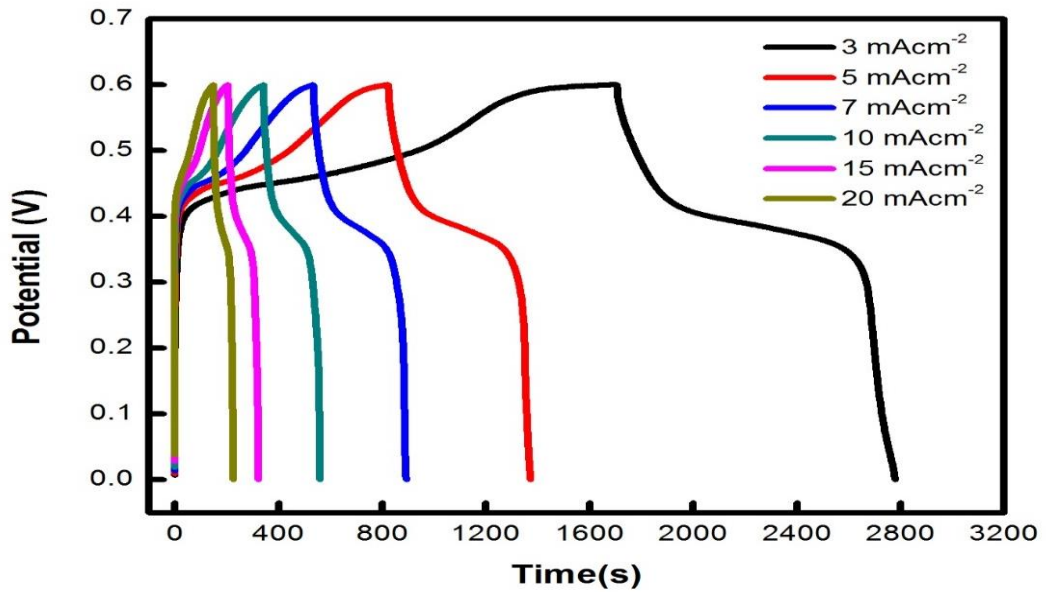


Figure 4.10 GCD curves for NiCo<sub>2</sub>S<sub>4</sub>/MWCNTs/Ni foam

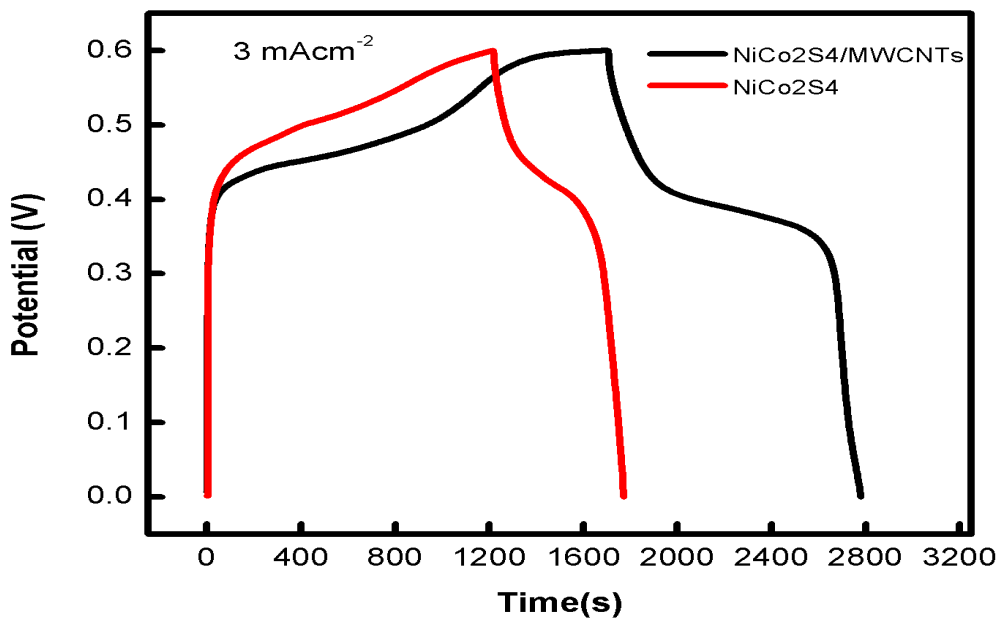


Figure 4.11 GCD comparison curves for NiCo<sub>2</sub>S<sub>4</sub> and NiCo<sub>2</sub>S<sub>4</sub>/MWCNTs

It is clear from the above figures that the NiCo<sub>2</sub>S<sub>4</sub>/MWCNTs has exceptionally higher charge /discharge time as related to its counterpart. This higher charge/discharge time accounts for the superior capacitance of nanocomposite over the NiCo<sub>2</sub>S<sub>4</sub> NSs. The improvement of capacitance in case of the nanocomposite can be credited to synergic effect produced from the combination of binary transition metal sulfide and carbon. Another important reason to this enhancement of capacitance is the improved faradic

process triggered by the presence of MWCNTs which acts a supporting highly conductive scaffold for the binary metal sulfide NSs.

For the sake to study discharge behavior of NiCo<sub>2</sub>S<sub>4</sub> NSs and NiCo<sub>2</sub>S<sub>4</sub>/MWCNTs nanocomposite GCD analysis was conducted at different current densities. The GCD measurements for both materials are experienced in a three electrode assembly. The discharge curves for the NiCo<sub>2</sub>S<sub>4</sub> NSs are given below.

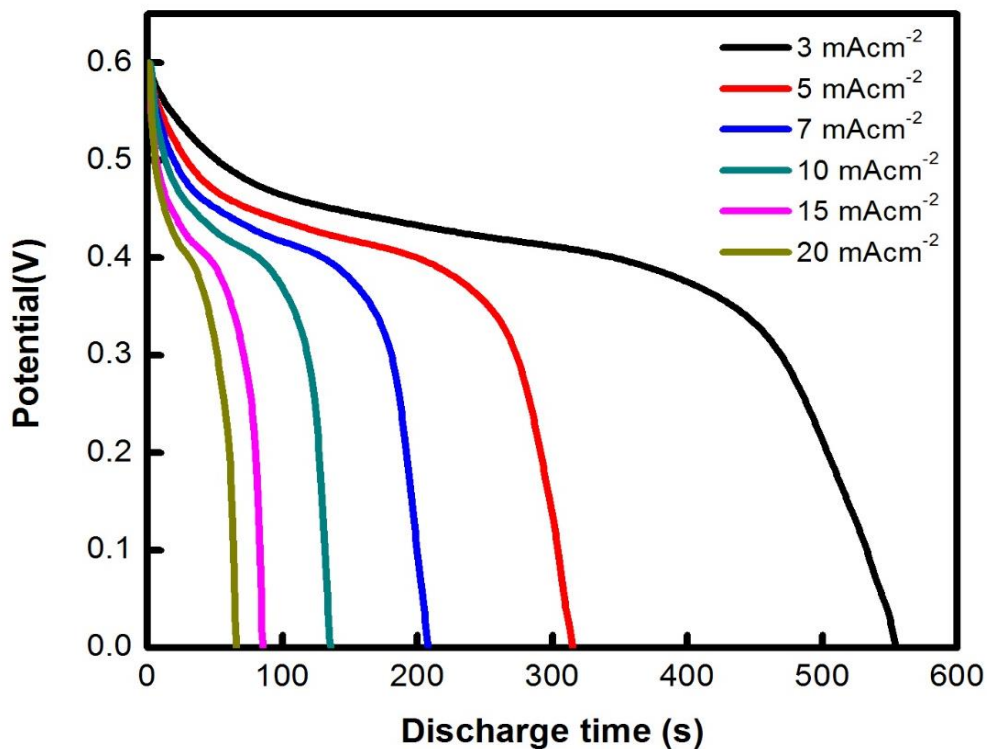


Figure 4.12 Galvanostatic discharge curves of NiCo<sub>2</sub>S<sub>4</sub> .

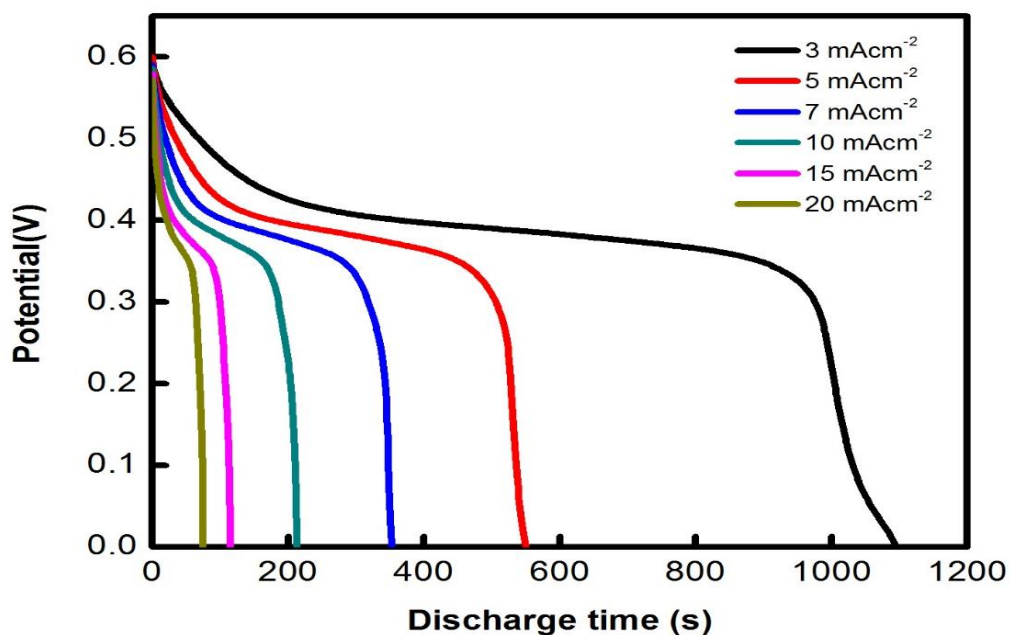


Figure 4.13 Galvanostatic discharge curves of NiCo<sub>2</sub>S<sub>4</sub> at different current rates

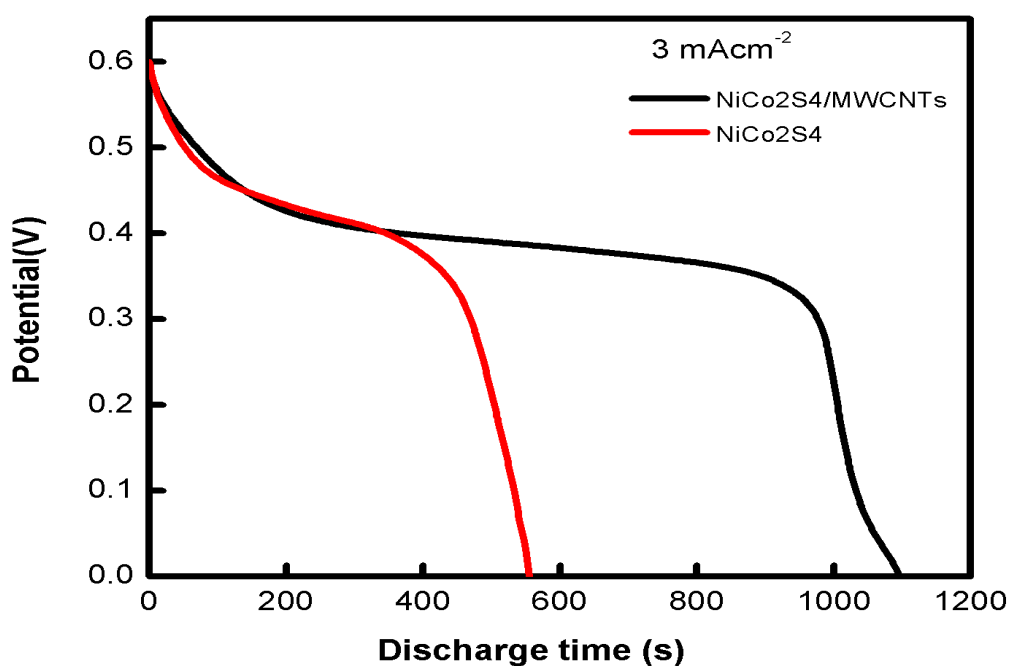


Figure 4.14 Galvanostatic discharge curves of NiCo<sub>2</sub>S<sub>4</sub> and NiCo<sub>2</sub>S<sub>4</sub>/MWCNTs

It is clear from the above figure that the NiCo<sub>2</sub>S<sub>4</sub>/MWCNTs has exceptionally higher discharge time (1077s) as compared to its counterpart which has discharge time of (551s) at the current density of 3mAcm<sup>-2</sup>. This higher discharge time accounts for the superior capacitance of nanocomposite over NiCo<sub>2</sub>S<sub>4</sub> NSs. A capacitance of

2210  $\text{Fg}^{-1}$  is recorded for nanocomposite  $\text{NiCo}_2\text{S}_4$ . The specific capacitance achieved for  $\text{NiCo}_2\text{S}_4$  NSs is  $1295 \text{ Fg}^{-1}$ . The improvement of capacitance in case of the nanocomposite can be credited to synergistic effect produced from combining binary transition metal sulfide and carbon. Another important reason to this enhancement of capacitance is the improved faradic process triggered by the presence of MWCNTs which acts a supporting highly conductive scaffold for the binary metal sulfide NSs. The mass specific capacitance calculated for various current rates is given below.

**Table No.1**

### Mass Specific Capacitance Calculation

Mass specific capacitance  $\text{NiCo}_2\text{S}_4$  electrode material

Current density $\text{mAcm}^{-2}$	Discharge time(s)	Mass of active material (g)	Potential window ( $\Delta V$ )	Capacitance $C = \frac{I\Delta t}{m\Delta v} \text{ Fg}^{-1}$
3	551	2.127	0.6	1295
5	314	2.127	0.6	1230
7	206	2.127	0.6	1129
10	133	2.127	0.6	1042
15	84	2.127	0.6	987
20	61	2.127	0.6	940

Mass specific capacitance  $\text{NiCo}_2\text{S}_4/\text{MWCNT}$ 's electrode material

Current density $\text{mAcm}^{-2}$	Discharge time(s)	Mass of active material (g)	Potential window ( $\Delta V$ )	Capacitance $C = \frac{I\Delta t}{m\Delta v} \text{ Fg}^{-1}$
3	1077	2.436	0.6	2210
5	548	2.436	0.6	1875
7	360	2.436	0.6	1724
10	219	2.436	0.6	1498
15	117	2.436	0.6	1201
20	77	2.436	0.6	1054

Figure 4.15 showing the mass specific capacitance at different current densities.

The areal capacitance for both types of electrode materials is given by the equation given below.

$$C = \frac{I\Delta t}{A\Delta v} \text{ (Fcm}^{-2}\text{)} \quad (4.6)$$

Where, current density (A) is represented by I, discharge time (s) by  $\Delta t$  and discharging window by  $\Delta V$ , A is the area of sample ( $\text{cm}^{-2}$ ).

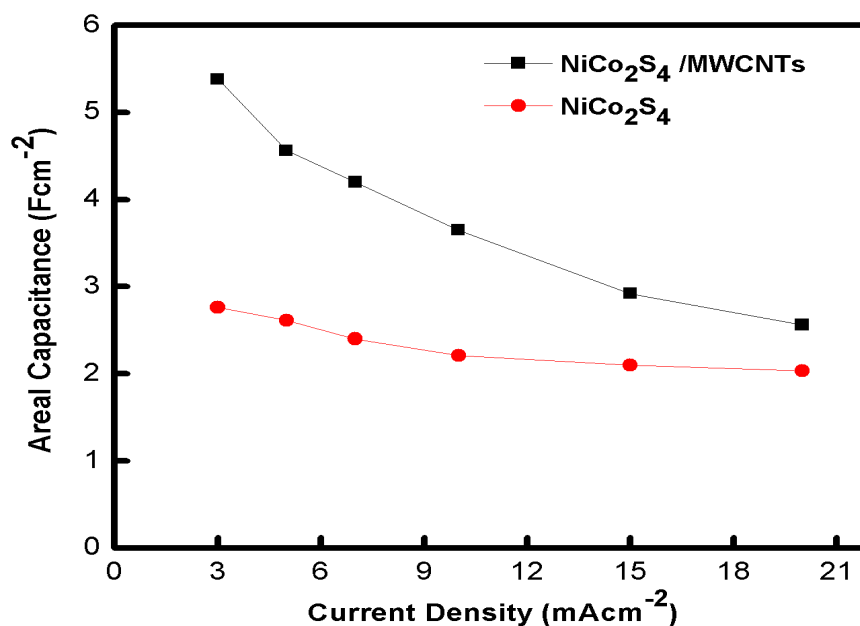


Figure 4.16 Areal capacitance vs current density

From the above graph it can be determined that NiCo<sub>2</sub>S<sub>4</sub>/MWCNTs material for electrode displays areal capacitance of 5.38 Fcm<sup>-2</sup>, while the NiCo<sub>2</sub>S<sub>4</sub> electrode material exhibits a areal capacitance 2.76 Fcm<sup>-2</sup> at scan rate of 3 mAcm<sup>-2</sup>. The areal capacitance in case of NiCo<sub>2</sub>S<sub>4</sub>/MWCNTs composite is almost 2 times higher as compared to only NiCo<sub>2</sub>S<sub>4</sub> electrode material. The areal capacitance of NiCo<sub>2</sub>S<sub>4</sub> material at current densities of 5, 7, 10, 15 and 20 mAcm<sup>-2</sup> is 2.61, 2.40, 2.21, 2.10 and 2.03 Fcm<sup>-2</sup> respectively. The areal capacitance of NiCo<sub>2</sub>S<sub>4</sub>/MWCNTs material at current densities of 5,7,10, 15 and 20 mAcm<sup>-2</sup> is 4.56, 4.20, 3.65, 2.92 and 2.56 Fcm<sup>-2</sup> respectively.

Moreover as current density is increased the areal capacitance was decreasing in both cases due to inaccessibility of electrolyte to all active sites of our material for the charge transportation.

In direction to examine cyclic stability of NiCo<sub>2</sub>S<sub>4</sub> NSs and NiCo<sub>2</sub>S<sub>4</sub>/MWCNTs nanocomposite GCD analysis was accompanied at a current rate of 20 mA cm<sup>-2</sup>. The GCD measurements for both the materials are conceded out in a three electrode system. The working potential window utilized for GCD analysis is 0.00 V to 0.6V. The stability of materials investigated via GCD analysis is presented below.



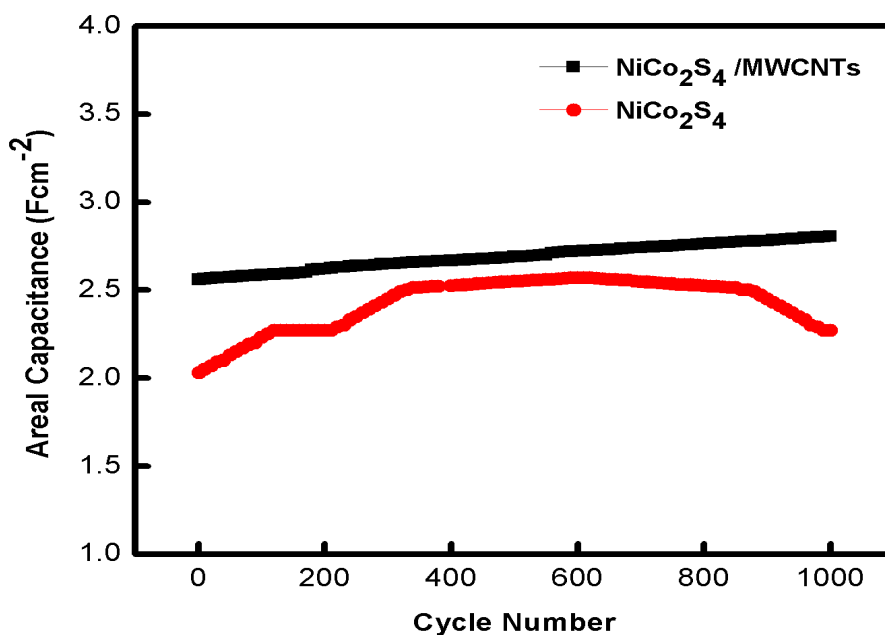


Figure 4.17 the cycling performance of NiCo<sub>2</sub>S<sub>4</sub>/MWCNTs/Ni and NiCo<sub>2</sub>S<sub>4</sub>/Ni electrodes at the current density of 20 mA cm<sup>-2</sup>.

The cycling performance for both type of electrode material was calculated by charging and discharging tests for 1000 times at the fixed current rate of 20 mA cm<sup>-2</sup>. As given in fig.4.17, the capacitances of two materials progressively increase due the activation of inner side material in initial stage. In case of NiCo<sub>2</sub>S<sub>4</sub>/MWCNTs/Ni electrode areal specific capacitance was increasing continuously during 1000 cycles. While in case of NiCo<sub>2</sub>S<sub>4</sub>/Ni electrode capacitance was increasing initially up to 600 cycles after this it started to decrease. Cyclic stability test shows that NiCo<sub>2</sub>S<sub>4</sub>/MWCNTs/Ni electrode has good cyclic stability as compared to NiCo<sub>2</sub>S<sub>4</sub>/Ni electrode.

## Conclusions

In this work, NiCo<sub>2</sub>S<sub>4</sub> /MWCNTs NSs on Ni foam have been synthesized by hydrothermal method involving two steps based on the ion-exchange response. The synthesis approach in this work is environmental affability and very effective. For comparison, the nanostructures of Ni-Co Sulfide on nickel foam is also deposited by the same approach. Both Ni- Co Sulfide and NiCo<sub>2</sub>S<sub>4</sub>/MWCNTs NSs are investigated as direct materials for electrode for supercapacitor. Remarkably, Ni-Co sulfide/MWCNTs electrode exhibits a high areal capacitance of 5.38 F cm<sup>-2</sup>. The corresponding mass specific capacitance at the current density of 3 mA cm<sup>-2</sup> was calculated 2210 F g<sup>-1</sup>.

Areal capacitance 2.76 F cm<sup>-2</sup> and mass specific capacitance of 1295 Fg<sup>-1</sup> for the Ni-Co sulfide electrode is calculated, which is lesser as compared to discussed earlier one. Moreover, the NiCo<sub>2</sub>S<sub>4</sub> /MWCNTs electrode also exhibits good rate capability and cycling stability. Keeping above in view it can be concluded that such Ni-Co sulfide/MWCNTs NSs can be used in supercapacitor applications. As a binder-free electrode for the fabrication of high performance energy storage devices. This work could make some contribution to synthesis the materials for high performance electrodes and the rational design.

## References

- [1] G. Z. Wang, L. Zhang, J., "A review of electrode materials for electrochemical supercapacitors," *Chem Soc Rev*, 2012.
- [2] Z. Chenguang Liu, David Neff, Aruna Zhamu and Bor Z. Jang, "Graphene-Based Supercapacitor with an Ultrahigh Energy Density," 2006.
- [3] C. M. K. Park, J. H. Kim, H. Sohn, H. J., "Li-alloy based anode materials for Li secondary batteries," *Chem Soc Rev*, Aug 2010.
- [4] H. Y. Wu, G. Pan, L. Liu, N., M. T. McDowell, Z. Bao, and Y. Cui, "Stable Li-ion battery anodes by in-situ polymerization of conducting hydrogel to conformally coat silicon nanoparticles," *Nat Commun*, vol. 4, p. 1943, 2013.
- [5] M. T. Armand, J. M., "Building better batteries," *Nature*, vol. NATURE|Vol 451|7 February 2008, 2008.
- [6] "Haosen Fan, ab Hao Wang, ab Ning Zhao, Xiaoli Zhanga and Jian Xu, Supercapacitor electrode materials, 2012.
- [7] L. Nyholm, G. Nystrom, A. Mihranyan, and M. Stromme, "Toward flexible polymer and paper-based energy storage devices," *Adv Mater*, vol. 23, pp. 3751-69, Sep 1 2011.
- [8] Chien, Wei-Yun Wang, Yong-Hui Lu, Shih-Yuan, "Ultrahigh Specific Capacitances for Supercapacitors Achieved by Nickel Cobaltite/Carbon Aerogel Composites," *Advanced Functional Materials*, 2012.
- [9] H. Jiang, P. S. Lee, and C. Li, "3D carbon based nanostructures for advanced supercapacitors," *Energy Environ. Sci.*, vol. 6, pp. 41-53, 2013.
- [10] X. M. You, Manjusri Gregori, Stefano and A. K. Mohanty, "Preparation of an Electric Double Layer Capacitor (EDLC) Using Miscanthus-Derived Biocarbon," *ACS Sustainable Chemistry & Engineering*, vol. 6, pp. 318-324, 2017.
- [11] J. R. Miller and P. Simon, "Materials science. Electrochemical capacitors for energy management," *Science*, vol. 321, pp. 651-2, Aug 1 2008.
- [12] M. C. R. Kötz, *Principles and applications of electrochemical capacitors*, *Electrochim. Acta*.

- [13] T. F. Zhenqi Guo, and Hengzhi Fu "C rystal Orientation Measured by XRD and Annotation of the Butterfly Diagram," MATERIALS CHARACTERIZATION 2000.
- [14] Chenguang Liu, Zhenning Yu, David Neff, Aruna Zhamu, and Bor Z. Jang, Graphene-Based Supercapacitor with an Ultrahigh Energy Density.
- [15] Y. Wang, Ken S.Mishler, Jeffrey Cho, Sung ChanAdroher, Xavier Cordobes, "A review of polymer electrolyte membrane fuel cells: Technology, applications, and needs on fundamental research," Applied Energy, 2011.
- [16] M. P. Lefevre, E. Jaouen, F. Dodelet,, "Iron-based catalysts with improved oxygen reduction activity in polymer electrolyte fuel cells," Science, 2009.
- [17] A. Burke, "R&D considerations for the performance and application of electrochemical capacitors," Electrochimica Acta, vol. 53, pp. 1083-1091, 2007.
- [18] A. Davies and A. Yu, "Material advancements in supercapacitors: From activated carbon to carbon nanotube and graphene," The Canadian Journal of Chemical Engineering, vol. 89, pp. 1342-1357, 2011.
- [19] R. Ko'tz a, M. Carlen b, " Principles and applications of electrochemical capacitors,Electrochim. Acta.pdf," Electrochimica Acta 45 (2000) 2483–2498.
- [20] A.D. Golub, "The electrical double layer of carbon and graphite electrodes Part V. Specific interactions with simple ions," 1988.
- [21] F. Lai, Y. E. Miao, L. Zuo, H. Lu, Y. Huang, and T. Liu, "Biomass-Derived Nitrogen-Doped Carbon Nanofiber Network: A Facile Template for Decoration of Ultrathin Nickel-Cobalt Layered Double Hydroxide Nanosheets as High-Performance Asymmetric Supercapacitor Electrode," Small, vol. 12, pp. 3235-44, Jun 2016.
- [22] R. R. Salunkhe, K. Jang, S.-w. Lee, S. Yu, and H. Ahn, "Binary metal hydroxide nanorods and multi-walled carbon nanotube composites for electrochemical energy storage applications," Journal of Materials Chemistry, vol. 22, p. 21630, 2012.
- [23] D. X. Kunfeng Chen, "Ionic Supercapacitor Electrode Materials: A System-Level Design of Electrode and Electrolyte for Transforming Ions into Colloids," Colloids and Interface Science Communications, 2014.
- [24] M. C. R. Kötzt, "Principles and applications of electrochemical capacitors," Electrochimica Acta, 2483–2498, vol. 2000.

- [25] Vinay Gupta, Norio Miura, "Influence of the microstructure on the supercapacitive behavior of polyaniline/single-wall carbon nanotube composites," *Journal of Power Sources* 2006.
- [26] S.Sarangapani, N. ICE1 Incorporated, Massachusetts 02062, USA, and P. Chen, "Theoretical and Experimental Constraints."
- [27] D. C. GRAHAME, "THE ELECTRICAL DOUBLE LAYER AND THE THEORY OF ELECTROCAPILLARITY'."
- [28] J. C. David Leonard Chapman, Oxford, "LI. A contribution to the theory of electrocapillarity," *Philosophical Magazine Series* 2010.
- [29] R. Ko'tz, M. Carlen, Principles and applications of electrochemical capacitors, *Electrochim. Acta.*, 1999.
- [30] M. FOLMAN, "THE ELECTRICAL DOUBLE LAYER OF HIGH SURFACE POROUS CARBON ELECTRODE," 1971.
- [31] S. Y OREN, "THE ELECTRICAL DOUBLE LAYER OF CARBON AND GRAPHITE ELECTRODES," *J Electroanal Chem*, 1984.
- [32] A. SOFFER, "THE ELECTRICAL DOUBLE LAYER OF CARBON AND GRAPHITE ELECTRODES," *J Electroanal Chem*, 186 (1985) 63-77, 1985.
- [33] B. Kastening, "A Model of the Electronic Properties of Activated Carbon."
- [34] Graeme A. Snook, Pon Kaob, Adam S. Bestb, "Conducting-polymer-based supercapacitor devices and electrodes " *Journal of Power Sources* 196 (2011) 1–12, 2011.
- [35] F. L. Ming Huang, Fan Dong, Yu Xin Zhang, and Li Li Zhang, "MnO<sub>2</sub>-based nanostructures for high-performance supercapacitors," *J. Mater. Chem.*, 2015.
- [36] J. C. Hao, "Fabrication of high-performance supercapacitors based on hollow SnO<sub>2</sub> microspheres," *J Solid State Electrochem*, 2013.
- [37] Q.Chunzhen Yang, "Three-dimensional ordered macroporous MnO<sub>2</sub>/carbon nanocomposites as high-performance electrodes for asymmetric supercapacitors " *Phys.Chem.*, 2013.
- [38] J. C. Myeongjin Kim, Ilgeun Oh and Jooheon Kim\*, "Design and synthesis of ternary Co<sub>3</sub>O<sub>4</sub>/carbon coated TiO<sub>2</sub> hybrid nanocomposites for asymmetric supercapacitors," *Physical Chemistry Chemical Physics*, 2012.
- [39] J. L. Shixiong Sun, Rutao Wang, Lingbin Kong, Xiaocheng Lia and Xingbin Yan, "Identifying pseudocapacitance of Fe<sub>2</sub>O<sub>3</sub> in an ionic liquid and its application in asymmetric supercapacitors," *J. Mater. Chem.*, 2014.

- [40] D. C. GRAHAME, "THE ELECTRICAL DOUBLE LAYER AND THE THEORY OF ELECTROCAPILLARITY'," THEORY OF ELECTROCAPILLARITY, 1947.
- [41] J. P. C. X.F.Gong, K.Y.Ma.,F.Liu, Li Zhang ,, XiaoBin Zhang "Nanostructured nickel-cobalt sulfide grown on nickel foam directly as supercapacitor electrodes with high specific capacitance," Materials Chemistry and Physics 2016.
- [42] L. C. Jun Ge, "Transparent and flexible electrodes and supercapacitors using polyaniline/ single-walled carbon nanotube composite thin film," Nanoscale, 2011,, 2011.
- [43] M. J. Kelly, "Cyclic Voltammetry," vol. Journal of Chemical Education.
- [44] M. Faisal ,Naeem Ashiq "High Specific Capacitance and Energy density of synthesizes AL<sub>2</sub>S<sub>3</sub> nanorambutan as electrode material for supercapacitor ."
- [45] M. V. S. T.C. Girija, "Analysis of polyaniline-based nickel electrodes for electrochemical supercapacitors " Journal of Power Sources 156 (2006) 705–711, 2005.
- [46] Chi-Chang Hu\*, Jeng-Yan Lin, "Effects of the loading and polymerization temperature on the capacitive performance of polyaniline in NaNO<sub>3</sub>," Electrochimica Acta 47 (2002).
- [47] V. K. E. Frackowiaka, K. Jurewicz, "Supercapacitors based on conducting polymers/nanotubes composites," Journal of Power Sources 153 (2006) 413–418, 2006.
- [48] V. K. K. Lotaa, E. Frackowiaka, "Capacitance properties of poly(3,4-ethylenedioxythiophene)/carbon nanotubes composites," Journal of Physics and Chemistry 2004.
- [49] Shu-Lei Chou, Jia-Zhao Wanga, Sau-Yen Chew, Hua-Kun Liu, Shi-Xue Dou, "Electrodeposition of MnO<sub>2</sub> nanowires on carbon nanotube paper as free-standing, flexible electrode for supercapacitors," Electrochemistry Communications.
- [50] P. S. Alexis Laforgue, "Polythiophene-based supercapacitors," Journal of Power Sources, 1999.
- [51] D. W. C. Liming Dai , Jong-Beom Baek , and Wen Lu "Carbon Nanomaterials for Advanced Energy Conversion and Storage," small 2012, 2012.

- [52] S.R. Sivakkumara, Ji-Ae Choia, Douglas R. MacFarlane b, and D.-W. K. Maria Forsyth, "Electrochemical performance of polyaniline nanofibres and polyaniline/multi-walled carbon nanotube composite as an electrode material for aqueous redox supercapacitors," *Journal of Power Sources*, 2007.
- [53] Shin-Ming Li, Yu-Sheng Wang, Shin-Yi Yang, Chia-Hong Liu, Kuo-Hsin "Electrochemical deposition of nanostructured manganese oxide on hierarchically porous graphene/carbon nanotube structure for ultrahigh-performance electrochemical capacitors," *Journal of Power Sources*, 2013.
- [54] M. C. Yunxia Huang, Zhongcheng Xiang and Yimin cui, "Facile synthesis of NiCo<sub>2</sub>S<sub>4</sub>/CNTs nanocomposites for high-performance supercapacitors," 2018.
- [55] A. G. Indrajit Shown, Li-Chyong Chen & Kuei-Hsien Chen, "Conducting polymer-based flexible supercapacitor " *Energy Science and Engineering*, 2015.
- [56] V. Khomenko, E. Frackowiak, F. B., "Determination of the specific capacitance of conducting polymer/nanotubes composite electrodes using different cell configuration," *Electrochimica Acta* 2005.
- [57] C. P. F. S. Neves, "Influence of template synthesis on the performance of polyaniline cathodes," *Journal of Power Sources* 107 (2002) 13–17, 2002.
- [58] Pawel J. Kulesza, Magdalena Skunika, Beata Baranowska, Krzysztof "Fabrication of network films of conducting polymer-linked polyoxometallate-stabilized carbon nanostructures " *Electrochimica Acta* 51 (2006) 2373–2379, 2006.
- [59] D. S. Jing Zhang, Shaolin Mu\*, "A rechargeable Zn- poly(aniline-co-m-aminophenol) battery " *Journal of Power Sources* 161 (2006) 685–691, 2006.
- [60] M. F. M. Hassan Karamia, \*, and M. Shamsipur, "A new design for dry polyaniline rechargeable batteries," *Journal of Power Sources* 117 (2003) 255–259, 2003.
- [61] Q. Wei Chen, Dongwook Chang, Liming Dai, Sabyasachi Ganguli and Ajit Roy, "Vertically-aligned carbon nanotubes infiltrated with temperature-responsive polymers: smart nanocomposite films for self-cleaning and controlled release," *Chemical communication* 2007.
- [62] H.-Q. L. By Yong-Gang Wang, and Yong-Yao Xia, "Ordered Whiskerlike Polyaniline Grown on the Surface of Mesoporous Carbon and Its Electrochemical Capacitance Performance," *Adv. Mater.*, 2006.

- [63] a. J. C. Yahya A. Ismail, b Su Ryon Shin, a Rajaram S. Mane, b Sung-Hwan Han, b, z and Seon Jeong Kima, z, "Hydrogel-Assisted Polyaniline Microfiber as Controllable Electrochemical Actuatable Supercapacitor," *Journal of The Electrochemical Society*, 2009.
- [64] B. N. Biplab K. Kuila, Marcus Bo' hme, Andreas Janke and Manfred Stamm, "Vertically oriented arrays of polyaniline nanorods and their super electrochemical properties," *Chem. Commun*, 2009.
- [65] J. M. Li-Zhen Fan, "High-performance polypyrrole electrode materials for redox supercapacitors," *Electrochemistry Communications*.
- [66] Y. W. Hongfang Ana, Xianyou Wanga, \*, Liping Zhenga, Xingyan Wanga, and L. B. Lanhua Yia, Xiaoyan Zhanga, "Polypyrrole/carbon aerogel composite materials for supercapacitor," *Journal of Power Sources* 195 (2010) 6964–6969, 2010.
- [67] Irin Sultanaa, M.M. Rahmana, Sha Lia, Jiazhao Wanga, Caiyun Wangb, G.G. Wallaceb, Hua-Kun Liua, "Electrodeposited polypyrrole (PPy)/para (toluene sulfonic acid) (pTS) free-standing film for lithium secondary battery application " *Electrochimica Acta* 60 (2012) 201– 205, 2012.
- [68] b. Jingping Wanga, Youlong Xu, Jie Wang Xianfeng Du, "Toward a high specific power and high stability polypyrrole supercapacitors," *Letter / Synthetic Metals*, 2011.
- [69] J. Y. M. Nakayama, K. Nakaoka, K. Ogura, "Electrodeposition of composite films consisting of polypyrrole and mesoporous silica," *Synthetic Metals* 128 (2002) 57–62, 2002.
- [70] Deepak P. Dubal, Jong Guk Kim, Won Bae Kim and Chandrakant D. Lokhande, "Porous polypyrrole clusters prepared by electropolymerization for a high performance supercapacitor," *J. Mater. Chem.*, 2011.
- [71] I. Z. X. Li, "Capacitive behaviour of polypyrrole films prepared on stainless steel substrates by electropolymerization," *Materials Letters*, 2012.
- [72] B. Y. Longyan Yuan, Bin Hu, Kaifu Huo, Wen Chenb and Jun Zhou, "Polypyrrole-coated paper for flexible solid-state energy storage," *Energy Environ. Sci.*, 2013.
- [73] b. Graeme A. Snook a, \*, George Z. Chen a, \*, "The measurement of specific capacitances of conducting polymers using the quartz crystal microbalance," *Journal of Electroanalytical Chemistry* 612 (2008) 140–146, 2008.



- [74] J. C. Weikuan Li, Junjun Zhao, Jianrong Zhang\*, Junjie Zhu, "Application of ultrasonic irradiation in preparing conducting polymer as active materials for supercapacitor " *Materials Letters*, 2005.
- [75] Keke Liu, Rong Xue, Jianrong Zhang\*, Junjie Zhu, "Electropolymerization of high stable poly(3,4-ethylenedioxythiophene) in ionic liquids and its potential applications in electrochemical capacitor " *Journal of Power Sources*, 2008.
- [76] A. T. P. Sivaraman, R. K. Kushwaha, D. Ratna, and A. B. Samuiz, "Poly(3-methyl thiophene)-Activated Carbon Hybrid Supercapacitor Based on Gel Polymer Electrolyte," *Electrochemical and Solid-State Letters*, 2006.
- [77] D. E. S. Anna M. Ö sterholm, Aubrey L. Dyer, and John R. Reynolds, "Optimization of PEDOT Films in Ionic Liquid Supercapacitors: Demonstration As a Power Source for Polymer Electrochromic Devices," *ACS Appl. Mater. Interfaces*, 2013.
- [78] J. T. K. a. M. E. Roberts, "Enhanced performance of triarylamine redox electrodes through directed electrochemical polymerization," *J. Mater. Chem.*, 2012, 22, 2392, 2012.
- [79] D. R. W. Mark E. Roberts, Bonnie B. McKenzie and Bruce C. Bunker, "High specific capacitance conducting polymer supercapacitor electrodes based on poly(tris(thiophenylphenyl)amine)<sup>†</sup>," *J. Mater. Chem.*, 2009, 19, 6977–6979, 2009.
- [80] Y.H.Lee, "Carbon-Based Electrochemical Capacitors," *ChemSusChem* 2012, 5, 480 – 499, 2012.
- [81] K. W. Jingjing Xu, Sheng-Zhen Zu, Bao-Hang Han, and Zhixiang Wei, "Hierarchical Nanocomposites of Polyaniline Nanowire Arrays on Graphene Oxide Sheets with Synergistic Effect for Energy Storage," *ACN NANO vol. VOL. 4 ▪ NO. 9 ▪ 5019–5026 ▪ 2010*, 2010.
- [82] Tzong-Ming Wu a, Yen-Wen Lin a, Chien-Shiun Liao b, "Preparation and characterization of polyaniline/multi-walled carbon nanotube composites," *Carbon* 2005.
- [83] G. C. Hao Zhang a, Zhiyong Wangb, Yusheng Yanga, Zujin Shi, Zhennan Gub, "Tube-covering-tube nanostructured polyaniline/carbon nanotube arraymmcomposite electrode with high capacitance and superior rate performance as well as good cycling stability," *Electrochemistry Communications* 10 (2008) 1056–1059.

- [84] J. L. Yueping Fanga, Deok Jin Yud, James P. Wickstedd, Kaan Kalkane, and B. N. F. C. Ozge Topale, JudyWuc, Jun Lia,\*, "Self-supported supercapacitor membranes: Polypyrrole-coated carbon nanotube networks enabled by pulsed electrodeposition," *Journal of Power Sources* 2009.
- [85] D. A. D. Sasha Stankovich<sup>1\*</sup>, Geoffrey H. B. Dommett<sup>1</sup>, Kevin M. Kohlhaas<sup>1</sup>, Eric J. Zimney<sup>1</sup>, and R. D. P. Eric A. Stach<sup>3</sup>, SonBinh T. Nguyen<sup>2</sup> & Rodney S. Ruoff<sup>1</sup>, "Graphene-based composite materials," Vol 442|20 July 2006|doi:10.1038/nature04969.
- [86] K. W. Jingjing Xu, Sheng-Zhen Zu, Bao-Hang Han, and Zhixiang Wei, "Hierarchical Nanocomposites of Polyaniline Nanowire Arrays on Graphene Oxide Sheets with Synergistic Effect for Energy Storage," *ACS NANO*, 2010.
- [87] P. A. Aaron Davies, Blake Farrow, Fathy Hassan, Zhongwei Chen, Ja-Yeon Choi, and Aiping Yu\*, "Graphene-Based Flexible Supercapacitors: Pulse-Electropolymerization of Polypyrrole on Free-Standing Graphene Films," *J. Phys. Chem. C* 2011, 115, 17612–17620, 2011.
- [88] F. L. Encarnacion Raymundo-Piñero, and François Béguin, "A High-Performance Carbon for Supercapacitors Obtained by Carbonization of a Seaweed Biopolyme, 2006 WILEY-VCH Verlag GmbH & Co. KGaA, Weinheim, 2006.
- [89] E. F. K. Kierzeka, G. Lotab, G. Gryglewicz, J. Machnikowskia, "Electrochemical capacitors based on highly porous carbons prepared by KOH activation," *Electrochimica Acta* 2004.
- [90] T. M. M. Endo, T. Takeda, Y. J. Kim, K. Koshiba, H. Hara, and M. S. Dresselhaus, "Capacitance and Pore-Size Distribution in Aqueous and Nonaqueous Electrolytes Using Various Activated Carbon Electrodes," *Journal of The Electrochemical Society*, 2011.
- [91] H. S. Deyang Qu "Studies of activated carbons used in double-layer capacitors," *Journal of Power Sources* 1998.
- [92] C. P. Celine Largeot, John Chmiola, Pierre-Louis Taberna, Yury Gogotsi, and Patrice Simon, "Relation between the Ion Size and Pore Size for an Electric Double-Layer Capacitor," *J. AM. CHEM. SOC.*, 2007.
- [93] L. D. a. Philippe Azaïs a, Pierre Florian b, Dominique Massiot b,, A. L.-S. c. Maria-Angeles Lillo-Rodenas c, Jean-Paul Peres d,, and F. o. B. e. a.

- Christophe Jehoulet, "Causes of supercapacitors ageing in organic electrolyte," *Journal of Power Sources* 171 (2007) 1046–1053, 2007.
- [94] A. S. Gregory Salitra, Linoam Eliad, Yair Cohen, and Doron Aurbach\*, "Carbon Electrodes for Double-Layer Capacitors I. Relations Between Ion and Pore Dimensions," *Journal of The Electrochemical Society*, 147 (7) 2486-2493 (2000), 2000.
- [95] D. H.-J. Mykola Seredycha, Gao Qing Lub, Teresa J. Bandosza., "Surface functional groups of carbons and the effects of their chemical character, density and accessibility to ion on electrochemical performance," *CA R B O N* 46 (2 008) 1475–1488, 2008.
- [96] K.-H. C. Hou-Sheng Huang , Norihiro Suzuki , Yusuke Yamauchi , and a. K. C.-W. W. Chi-Chang Hu "Evaporation-Induced Coating of Hydrous Ruthenium Oxide on Mesoporous Silica Nanoparticles to Develop High-Performance Supercapacitors," *small*
- [97] A. C. R. R.K. Sharma, S.B. Desu\*,1, "Manganese oxide embedded polypyrrole nanocomposites for electrochemical supercapacitor," *Electrochimica Acta* 53 (2008) 7690–7695, 2008.
- [98] Y. C. Ye Hou, Tyler Hobson, and Jie Liu, "Design and Synthesis of Hierarchical MnO<sub>2</sub> Nanospheres/Carbon Nanotubes/Conducting Polymer Ternary Composite for High Performance Electrochemical Electrodes," *Nano Lett.*, 2010.
- [99] C. Y. Zijin Su, Chengjun Xu, Haoyi Wu, Zhexu Zhang, Ting Liu, Chen Zhang, b Quanhong and a. Yang, b Baohua Li, a Feiyu Kang, "Co-electro-deposition of the MnO<sub>2</sub>/PEDOT:PSS Nanostructured Composite for High Areal Mass, Flexible Asymmetric Supercapacitor Devices," *Journal of Materials Chemistry*
- [100] Jianfeng Zang, Shu-Juan Bao, Chang Ming Li, Haijiao Bian, Xiaoqiang Cui,† and C. Q. S. Qiaoliang Bao, Jun Guo, and Keryn Lian|, "<Well-Aligned Cone-Shaped Nanostructure of Polypyrrole/RuO<sub>2</sub> and Its Electrochemical Supercapacitor." *American Chemical Society*, 2008.
- [101] S. B. Lee\*, "MnO<sub>2</sub>/Poly(3,4-ethylenedioxythiophene) Coaxial Nanowires by One-Step Coelectrodeposition for Electrochemical Energy Storage " *J. AM. CHEM. SOC.* 2008.
- [102] Y. Y. Peixu Li, Enzheng Shi, Qicang Shen, Yuanyuan Shang, Shiting Wu, Jinquan Wei, and H. Z. Kunlin Wang, "Core-Double-Shell, Carbon

- Nanotube@Polypyrrole@MnO<sub>2</sub> Sponge as Freestanding, Compressible Supercapacitor Electrode " ACS Appl. Mater. Interfaces.
- [103] L. W. Xiangcun Li, Jianhang Shi, Naixu Du, and Gaohong He, "Multishelled Nickel-Cobalt Oxide Hollow Microspheres with Optimized Compositions and Shell Porosity for High-performance Pseudocapacitors " ACS Appl. Mater. Interfaces.,, 2016.
- [104] H. B. W. Changzhou Yuan, Yi Xie,\* and XiongWen (David) Lou\*, "Mixed Transition-Metal Oxides: Design, Synthesis, and Energy-Related Applications " Angew. Chem. Int. Ed., 2014.
- [105] G. W. Anjon Kumar Mondal, Dawei Su, "Mesoporous MnCo<sub>2</sub>O<sub>4</sub> with a Flake-Like Structure as Advanced Electrode Materials for Lithium-ion batteries and Supercapacitors," Chem. Eur. J. 2014, 20,1 – 8, 2014.
- [106] L. H. Hao Chen , Min Chen , Yan Yan , and Limin Wu \*, "Nickel–Cobalt Layered Double Hydroxide Nanosheets for High-performance Supercapacitor Electrode Materials," 2013.
- [107] H. Z. Xin Xu , Shujiang Ding , Jun Li , Beibei Li , Demei Yu, "The facile synthesis of hierarchical NiCoO<sub>2</sub> nanotubes comprised ultrathin nanosheets for supercapacitors," Journal of Power Sources 2014
- [108] J. X. Yan Zhang, , Yayun Zheng, Yingjiu Zhang , Xing Hu and Tingting Xu, "NiCo<sub>2</sub>S<sub>4</sub>@NiMoO<sub>4</sub> Core-Shell Heterostructure Nanotube Arrays Grown on Ni Foam as a Binder-Free Electrode Displayed High Electrochemical Performance with High Capacity," Nanoscale Research Letters, 2017.
- [109] M. F. PingWen, Desuo Yang , YanWang , Hualei Cheng , JinqingWang "An asymmetric supercapacitor with ultrahigh energy density based on nickle cobalt sulfide nanocluster anchoring multi-wall carbon nanotubes hybrid," Journal of Power Sources 2016.
- [110] F. S. A. S. FATIKOW, "Smart Flexible Microrobots for Scanning Electron Microscope (SEM) Applications," JOURNAL OF INTELLIGENT MATERIAL SYSTEMS AND STRUCTURES, , vol. Vol. 11—March 2000, 2000.
- [111] F. A. Lixin DONG\*, and Toshio FUKUDA \*\*, "3d-nanorobotic-manipulation-of-nanoorder-objects-inside-sem," 2000 INTERNATIONAL SYMPOSIUM ON MICROMECHATRONICS AND HUMAN SCIENCE, 2000.

- [112] C.-H. W.X.-P. Jingw, "XRD and Raman Studies on the Ordering/Disordering of Ba(Mg<sub>1/3</sub>Ta<sub>2/3</sub>)O<sub>3</sub> " J. Am. Ceram. Soc, 2009.
- [113] F. d. O. A. João Victor Marques Zoccal<sup>a</sup>, José Antonio Silveira Gonçalves, "SYNTHESIS AND CHARACTERIZATION OF TiO<sub>2</sub> NANOPARTICLES BY THE METHOD PECHINI," Materials Science 2010.
- [114] J. B. Z. a. R. M. W. Kirk T. Kawagoe, "Principles of voltammetry and microelectrode surface states," Journal of Neuroscience Methods, 48 (1993) 225-240, 1993.
- [115] A. S. E. a. D. J. Kang\*, "Synthesis and characterization of CuO nanowires by a simple wet chemical method," Ethiraj and Kang Nanoscale Research Letters 2012, 7:70, 2012.
- [116] X. L. Li, Q.Wu, Y.Rui, M.Zeng, H., "Two-Dimensional, Porous Nickel-Cobalt Sulfide for High-Performance Asymmetric Supercapacitors," ACS Appl Mater Interfaces, 2015.